UNIVERSITÀ DI PISA

DIPARTIMENTO DI INGEGNERIA MECCANICA, NUCLEARE E DELLA PRODUZIONE

ANALYSIS OF THE EXTERNAL RADIOACTIVE RELEASES FOR AN IN-VESSEL BREAK IN THE POWER PLANT CONCEPTUAL STUDY USING THE ECART CODE

S. Paci

DIMNP 022 (03)

Work performed for ENEA Thermonuclear Fusion Division in the framework of the Contract No. 03/58/30/AA (Prot. 244/FUS-STG/ac)

SUMMARY

In the present report the work carried out by the DIMNP of Pisa University for ENEA-CR Frascati in the framework of the Contract ***No. 03/58/30/AA (Prot. 244/FUS-STG/ac)*** *is presented. This work is related to the application of the CESI and EdF ECART code on the analysis of the tritium and dusts external releases for an in-vessel break in the helium cooling loop of the first wall / blanket for the Power Plant Conceptual Study (PPCS). In particular the influence on the releases of a Detritiation System (DS) and of a dust scrubber with constant decontamination factor, not implemented in the original PPCS design, are analysed. Furthermore, some parametrical analysis on the influence, on the external releases, of the mass fraction of dust resuspended inside the VV at the beginning of the sequence have been also performed.*

These analyses are the follow-up of a previous DIMNP study about the phenomenological behaviour of the PPCS containment (vacuum vessel walls and expansion volume walls), giving the first indications on the amount of the external radioactive releases.

The activities have been also carried out in the general framework of the validation phase of the ECART code, initially developed for integrated analysis of severe accidents in LWRs, for its application on incidental sequences related to fusion plants. ECART was originally designed and validated for safety analyses of fission NPPs and is internationally recognized as a relevant nuclear source term code for these fission plants. It permits the simulation of chemical reactions and transport of radioactive gases and aerosols under two-phase flow transients in generic flow systems, using a built-in thermal-hydraulic model.

INDEX

Index of Tables

Index of Figures

Acronyms

ACP	Activated Corrosion Product
AMMD	Aerosol Mass Median Diameter
AV	Aerosol and Vapour
BL	Blanket
CH	Chemical
DBA	Design Basis Accident
DIMNP	Dipartimento di Ingegneria Meccanica, Nucleare e della Produzione
DS	Detritiation System
DV	Divertor
EdF	Electricité de France
ENEA	Ente per le Nuove Tecnologie l'Energia e l'Ambiente
EU	European Union
EV	Expansion Volume
EVITA	Experimental Vacuum Ingress Test Apparatus
FEAT	Fusion Energy Amplifier Tokamak
FPSS	Fast Plasma Shutdown System
FW	First Wall
GSSR	ITER Generic Site Safety Report
HTS	Heat Transport System
HX	Heat Exchanger
ICE	Ingress of Coolant Event
ITER	International Thermonuclear Experimental Reactor
LOCA	Loss Of Coolant Accident
LOVA	Loss Of Vacuum Accident
LWR	Light Water Reactor
NPP	Nuclear Power Plant
PFC	Plasma Facing Component
PPCS	Power Plant Conceptual Study
PS	Primary System
RCS	Reactor Cooling System
RD	Rupture Disk
SA	Severe Accident
TH	Thermal-Hydraulic
VV	Vacuum Vessel

1. INTRODUCTION

In the present Report DIMNP 022 (03) the work carried out by the Department of Mechanical, Nuclear and Production Engineering (DIMNP) of the UNIVERSITÀ DI PISA for the ENEA Fusion Division of Frascati (Rome) in the framework of the Contract **No. 03/58/30/AA (Prot. 244/FUS-STG/ac)** is presented. This work is related to the application of the ENEL (now CESI[1]) and EdF ECART (ENEL Code for Analysis of Radionuclide Transport) code [Parozzi, 1997a and 1997b] on a sequence of "in-vessel break" in the PPCS FW/BL cooling loop. In particular the influence on the radioactive releases of a DS and of a dust scrubber, not implemented in the original PPCS design, are analysed. Furthermore, some parametrical analysis on the influence, on the external dust releases, of the mass fraction of dust resuspended inside the VV at the beginning of the sequence have been also performed, being the dust resuspension phenomenology inside a very low pressure volume, as the VV of a fusion plant, an open safety issue [Porfiri, 2003a].

These activities have been also carried out in the general framework of the ECART validation phase, being the code initially developed by ENEL and EdF for integrated analysis of SAs in LWRs, for its application on incidental sequences related to the ITER FEAT fusion plant. Main points of this validation phase for the thermal-hydraulic module were, in the past, the DIMNP activities related on the Japanese ICE facility [Oriolo, 1998] and on the French EVITA experimental apparatus [Paci, 2000], always performed in the framework of research contracts between Pisa University and ENEA Frascati.

All the related geometrical data and the specific initially and boundary conditions for the analysis have been furnished to the DIMNP by ENEA Frascati Fusion Division [Di Pace, 2002], [ENEA, 2003], [Meloni, 2003] while the ECART code was made available to ENEA Frascati and Pisa University by CESI Milan.

To select the PPCS accident analyses to be analysed the following criterion was followed [Di Pace, 2002]: selection of accidents **involving phenomena or evaluation of parameters not yet studied** in the previous safety reactor studies. In particular, the first chosen sequence was a "*total LOFA in the primary loop followed by an in vessel LOCA without plasma shutdown*". The frequency of this

[1] CESI acquired at the end of 1999 the Research & Development division of ENEL.

accident chain is low because the pump stop is easily detectable as well as overpressurization of primary loop and, finally, because both active and passive shutdown systems could intervene to avoid the melting of PFCs. In any case, such a sequence was studied to test capability of mitigating systems (e.g.: pressure suppression systems, isolation systems, etc.) to operate also in such conditions, avoiding challenging of containments and possible radioactive release. In the present work, as required by the ENEA contract, only this **LOFA followed by an in-VV LOCA for Model B** of PPCS (helium cooled) has been analysed using ECART.

This report DIMNP 022 (03) contains the ECART analyses particularly focused on the tritium and dusts releases estimation, that is the follow-up of a previous DIMNP study [Paci, 2003] about the phenomenological behaviour of the PPCS containment (formed by the VV and EV walls). The previous work was performed because the EV free volume and other parameters of the PPCS confinement were not yet defined inside the PPCS design and the previous ECART analyses have given indications on the main values significant for what is concerning public safety, e.g.: free volumes of the system, set point of the rupture disk, leakage rates and ventilation systems, etc. The cited design parameters are significant to keep maximum pressures inside PPCS containment volumes below their design values, to avoid breaks in the PPCS confinement **but not to avoid large radiological releases** [Paci, 2003] even if PPCS confinements maintain their integrity in case of accident. For this reason, the present activities on the influence on the external radioactive releases of possible mitigation actions to be included in the PPCS design (as a DS or a scrubber) have been carried out.

2. OVERVIEW OF ECART MODELS

2.1 Main Features of the Code

ECART is designed [Parozzi, 1997a and 1997b] to operate with three sections (Figure 2.1), linked together, but able to be activated also as stand-alone modules:

1. **thermal-hydraulic (th)-** providing boundary conditions for chemistry and aerosol/vapour transport models;
2. **aerosol and vapour (av)-** calculating the amount of radioactive or toxic substances that may be retained or released in the analyzed circuit components;
3. **chemical (ch)** - chemical equilibrium among the compounds (only in vapour form) and reactions between gaseous phase and solid materials.

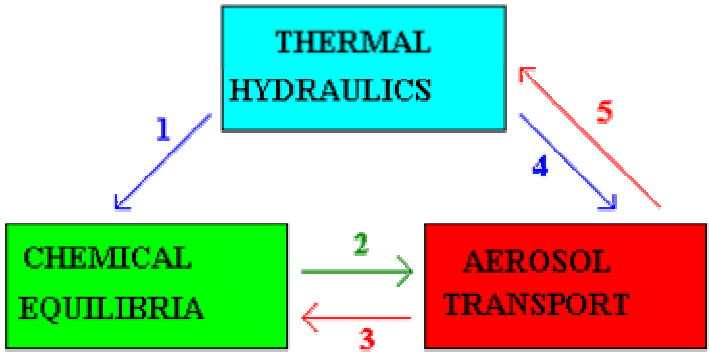

Figure 2.1: Schematic of the linking among the three main sections of ECART.

1. *thermal-hydraulic boundary conditions for chemical reactions*
2. *quantity of each chemical compound in gaseous phase*
3. *concentration of airborne reactants*
4. *thermal-hydraulic boundary conditions for aerosol and vapours transport phenomena*
5. *heat sources associated to transported species and aerosol concentrations capable to modify gas physical properties*

The code applies to pure transport phenomenology (mass, energy, momentum transfer and chemical processes) in whatever part of a given circuit. Support by other tools or experimental data can be used as boundary conditions or to account plant-dependent phenomena (e.g. releases from fuel, intervention of specific safety devices, etc.).

The ECART structure is designed to treat the thermal-hydraulic phenomena and the aerosol/vapour transport in an arbitrary flow system that the user can arbitrarily subdivide into a series of control volumes connected by flow junctions, chosen on the basis of considerations regarding geometrical features, thermal-hydraulic conditions and/or the expected retention of aerosols and vapours. Other details of transport analysis can be also decided by the user, like the number of chemical species, the occurrence of agglomeration or other phenomena and the multicomponent description.

Inside each control volume, a *two-region model* is adopted (Figure 2.2), being the liquid pool separated from the atmosphere. Within each region, thermal equilibrium is always assumed. Therefore, non-equilibrium effects related to superheated vapour injected in the pool or subcooled water sprayed in the atmosphere are separately accounted for.

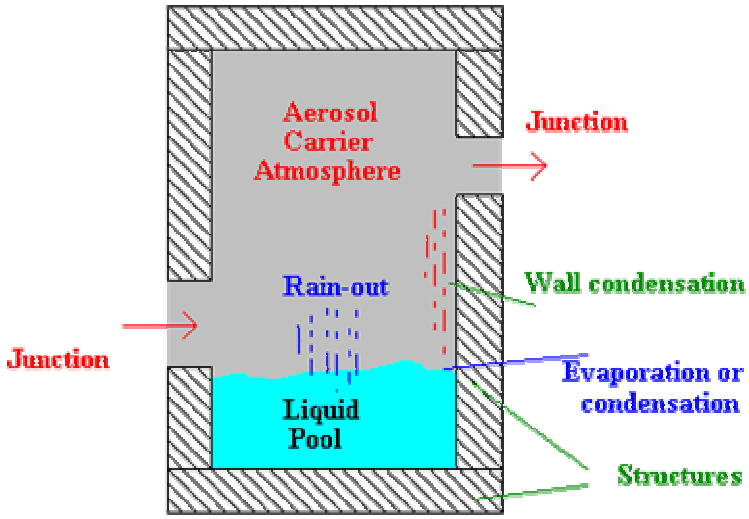

Figure 2.2: Control volume model adopted for ECART thermal-hydraulics.

Aerosols are assumed to be *well-mixed* inside the volumes. This assumption requires that the amount of vapour and/or aerosol removed within the control volume is “small” in relation to the total amount of material transported throughout the control volume itself. A corrective action (called “*plug*” flow) is provided for those volumes, like a long pipe, having only a radial mixing (a concentration gradient exists along the pipe). The direction and the rate of the carrier flow can be directly assigned in input, together with other boundary data, or can be predicted by the **th** section. This direction can change with time, although the aerosol transport through junctions is treated as one-dimensional (i.e. there is not simultaneous mixing through a junction). Two-dimensional flows,

required to simulate scenarios where the natural convection streams could enhance the mixing among the volumes, can be accounted using two junctions to describe the exchanges between the two volumes. Recirculation phenomena or chimney-effects promoted by the injection of hot or lighter gas into large environments are taken into account by **av** module, in the absence of any sub-nodalisation, through the estimate of a "recirculation velocity".

2.1.1 Thermal-Hydraulic Models

Basing on previous DIMNP experience in the development & application of models for analyzing thermal-hydraulics during postulated accidents and considering the peculiarities of the **av** models, the following characteristics were established for the **th** section [Ambrosini, 1995]:

- capability of describing **th** accident transients in NPP circuits, with the degree of detail required by the **av** section, and capability of processing incomplete experimental data providing the lacking information on local behaviour;
- transport simulation of the aerosol carrier gases expected within LWR plants under SA conditions and usually employed in experimental tests (steam, argon, helium, hydrogen, carbon dioxide, carbon monoxide, krypton, nitrogen, oxygen and xenon);
- solution of mass, energy and momentum balance equations in order to provide for realistic representations of fluid flow and heat transfer;
- calculation of pool levels in the control volumes and evaluation of steam suppression effects to support the aerosol scrubbing phenomenology;
- steam condensation modelled by splitting bulk and wall condensation (influencing, respectively, aerosol growth and aerosol diffusiophoretic deposition);
- allowance for counter-current flow conditions at junctions;
- capability of evaluating wall heat transfer taking into account wall thermal conductivity changes due to aerosol deposition and radioactive decay heat sources;
- possibility of characterizing heat structure surfaces with local hydraulic parameters having strong influence on aerosol deposition and resuspension mechanisms (i.e. hydraulic diameter, local fluid velocity and Reynolds number, etc.).

The assumption of complete stratification in a control volume is fairly well suited for containment analyses. It has some limitations in pipelines, but these limitations are accepted considering that, under SA conditions, single-phase flow (superheated steam-hydrogen mixture) or stratified flow (formation of water sumps in cold components) is likely to occur. A complete solution of the problem would require flow regime maps and constitutive laws for interfacial area and heat transfer under various regimes. However, this kind of accident scenarios, expected to be of minor importance in terms of Source Term (as a Steam Generator Tube Rupture), would imply removal mechanisms differing from those mainly influencing the Source Term associated to the SAs normally considered for probabilistic safety assessments.

2.1.2 Aerosol and Vapour Models

Although ECART adopts the classic well-mixed assumption to describe the transport within each control volume, the vapour and particles deposition and resuspension phenomena can be described by dividing each control volume into sub-regions (normally, coincident with single heat structures or sumps), where local thermal-hydraulic conditions (temperature, gas flow velocity, etc.) can be taken into account. By this way, small components or devices can be analyzed as part of larger control volumes, with a unique run of the master aerosol equation and longer time steps. Within each control volume, all phenomena that can be responsible for retention or re-entrance of radioactive or toxic substances can be taken into account (Figure 2.3).

Transport of volatile substances

Because of their negligible latent heat, condensation and evaporation of volatile species onto and from airborne particles and structure surfaces are dynamically calculated by diffusion equations. Conversely, steam-water phase changes can be either calculated by the **th** module or assigned as input. The condensation and evaporation onto and from airborne particles promote aerosol growth or shrinkage, modify the two shape factors if necessary (see next paragraph) while the presence of a liquid phase in an aerosol deposit can inhibit its resuspension.

Irreversible sorption of CsOH, I, I_2, HI, Te and Te_2 vapours onto wall surfaces (made by SS or nickel alloys) and airborne particles is also modelled by adopting experimentally based correlations. The experimentally determined vapour deposition velocities on hot surfaces may not represent an accurate description of the process as it occurs because of the imprecision in the available data [Parozzi, 1997b].

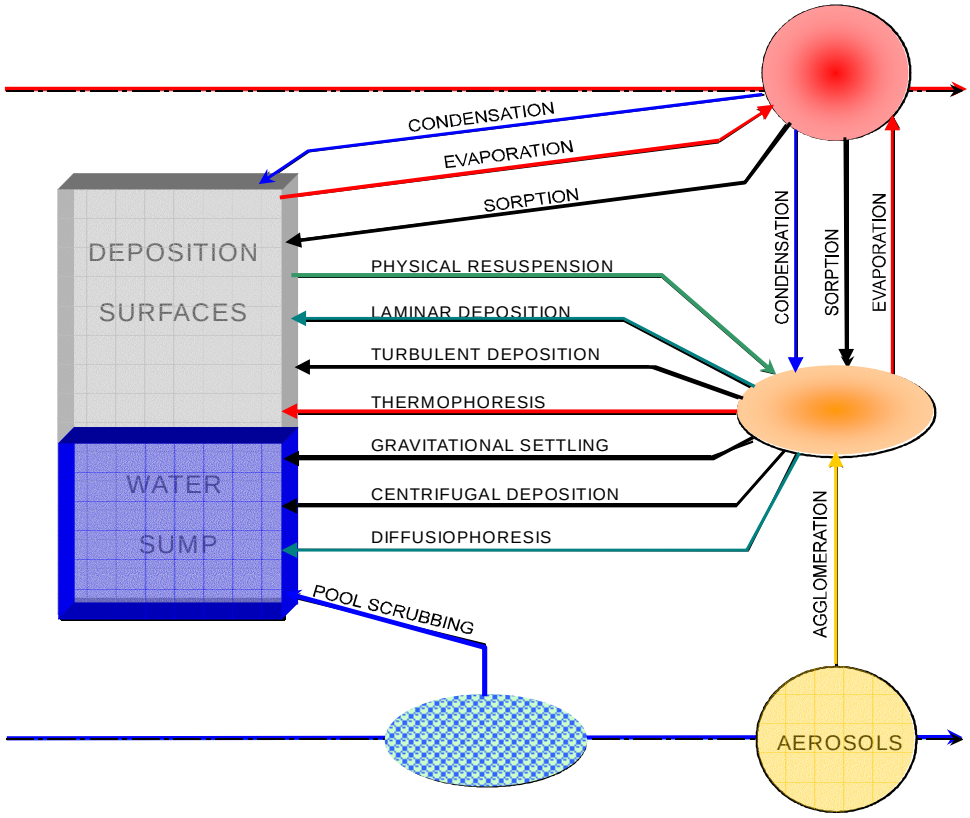

Figure 2.3: Aerosol and vapour transport phenomena simulated in each control volume.

Transport of aerosol particles

ECART works with discretised size distributions (Figure 2.4), both for airborne and deposited particles, where the maximum number of the size bins is an input choice (default 20). Ordinary differential equations solvers, with implicit integration methods, allow saving computing time and preventing numerical instabilities.

To compute the evolution of aerosol particles, mono-component basic aerosol equations can be used as default choice (i.e., at a given time, all the size bins in a given volume have the same composition). A multicomponent description of both airborne and deposited particles is possible optionally. This multicomponent approach (i.e., each size bin has its own composition), is obtained through an approximation: the **av** module individually tracks the transported species in each size bin, accounting for sources, particle growths or shrinking, depositions, resuspension, etc.. The correctness and the stability of this multicomponent approach were tested through virtual tests having a known solution.

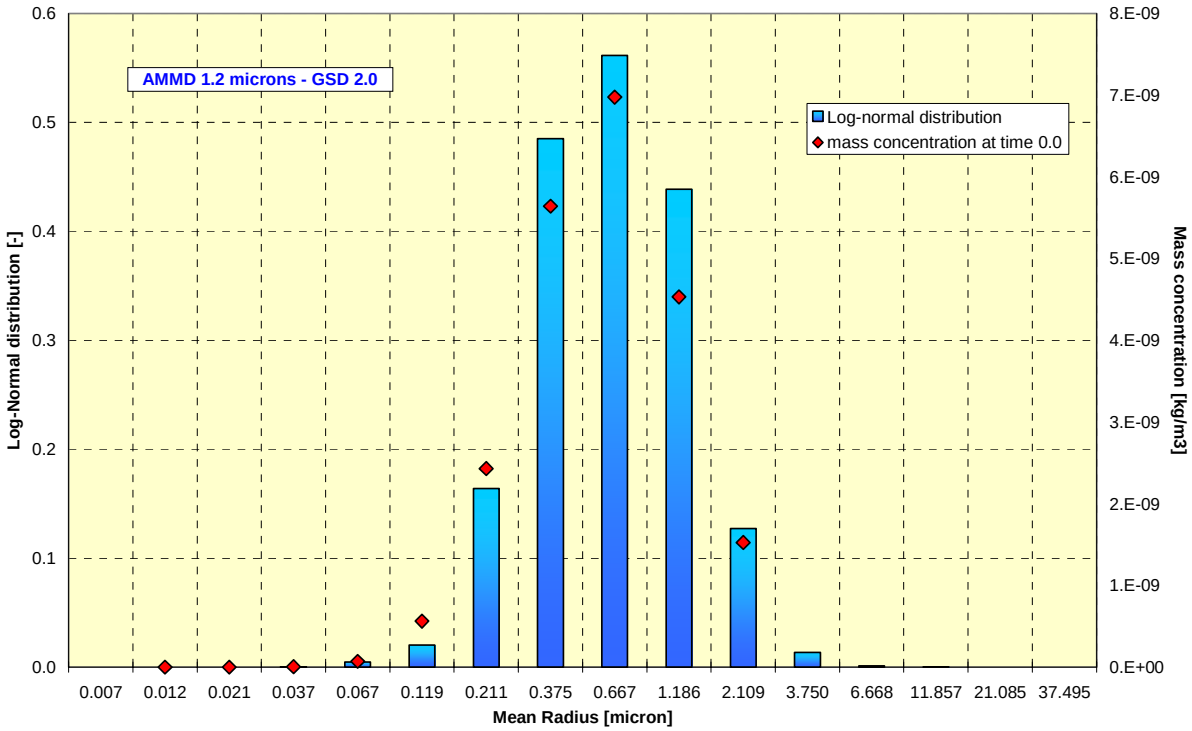

Figure 2.4: Aerosol particle size distribution modelled by ECART at a given time.

The asphericity of aerosol or dust particles is simulated by input assigning two size-dependent shape factors:

- "*aerodynamic shape factor*" χ, accounting for the different resistance to the motion of the actual particle if compared to the mass-equivalent sphere;
- "*collision shape factor*" γ, accounting for the increased effective collision cross-section.

The spherical shape is the code default for the particles (χ = 1.0 and γ = 1.0) but larger values for these two shape factors are normally present in LWR RCS conditions for "*dry*" particles [Brockmann 1985]. This spherical shape is however always assumed for "*wet*" particles, having an input given mass fraction of water (default 0.7), while the "dry factors are utilised if the liquid mass fraction is lesser than 0.2; for intermediate values a linear interpolation is performed.

The agglomeration models are based on the calculation of "*collision kernels*" related to the different mechanisms for the agglomeration of the airborne particles. The collision frequency is then calculated multiplying this kernel by the aerosol concentration. Three processes of agglomeration are taken into account:

1. Brownian (formula derived by Smoluchowski);
2. Gravitational (collision between particles having different settling velocities);
3. Turbulent, shear and inertial (Saffman and Turner's formula).

Particle growth due to bulk condensation of vapours and steam is modelled, also allowing the simulation of a possible hygroscopic behaviour of particles through the Van't Hoff factor, characterising the hygroscopicity of the considered chemical species. The Kelvin effect is taken into account in the case of steam condensation, which is inhibited for particles having radii smaller than the critical radius calculated by the code.

The deposition rate of the aerosol particles onto the different wall or pool surfaces is calculated as the sum of "deposition velocities" attributed to different effects:

- inertial impaction from turbulent flow (according to Liu-Agarwal observations);
- diffusion from turbulent flow (Davies' formula);
- diffusion from laminar flow (Gormley-Kennedy's formula);
- thermophoresis (Brock's correlation with Talbot's coefficients);
- gravitational settling (Stokesian and non-Stokesian regimes);
- centrifugation in curved pathways and pipe bends (Stokesian and non-Stokesian regimes; trapping in narrow bends);
- diffusiophoresis (Schmitt-Waldmann's formula).

The particle mechanical resuspension and the inhibition of their deposition, both caused by fast gas flows, is evaluated though an original semi-empirical approach based on a relationship between the acting forces on particles (adhesive and aerodynamic) and resuspension rates experimentally measured. This model takes into account both for the transient resuspension of already formed aerosol deposits and for the steady-state resuspension occurring in equilibrium with particle turbulent deposition.

In water sumps, the possible particle scrubbing phenomena is modelled, as described in the next Paragraph 2.1.2.1, accounting for the aerosol phenomena occurring within the rising bubbles: inward and condensing steam, gravitational settling, particle diffusion and centrifugation.

Coupling between aerosol and thermal-hydraulic calculations

In the case of a coupled run of aerosols and thermal-hydraulics, the **av** section receives all the required data from **th**, and gives a feedback to heat and mass transfer calculations. Then, the influence of high airborne aerosol concentrations on the gas physical properties (apparent density and viscosity) is taken into account.

The coupling among the two sections is explicit: as the **th** section and the **av** section are advanced with their own convergence criteria, a proper logic of time step synchronization is adopted. The thermal-hydraulic problem is firstly solved over the time interval between two synchronous conditions (of the order of the lowest Courant limit in the nodalisation), often adopting short time steps, suitable for numerical explicit algorithms. The aerosol calculations follow, with implicit integration methods allowing time steps usually an order of magnitude longer than the thermal-hydraulics ones: this technique gives the possibility to smooth out the data related to flow rates and pressures calculated by the **th** section in the case of oscillations due to limited instabilities.

2.1.2.1 Pool Scrubbing of Aerosols

The bubbling through water sumps is modeled by dividing the bubble evolution in two main zones: the injection zone and the bubble rise one. Within the injection zone, large globules are formed at the injection outlet; these globules can be unstable, but their break-up is not allowed within this first zone. Early condensation of steam is assumed to occur at the inlet of this zone (the bubble attains thermal equilibrium as it enters the pool), described in the code by only one axial step. Several steps, determined by a built-in criterion, are used on the contrary to model the bubble rise zone, where the rising bubble grows because of depressurization and steam evaporation; if unstable conditions are reached, the bubble break-up is also modeled (Figure 2.5). Depending on the pool depth, this second zone can represent either most of the bubble pathway or it can be completely absent.

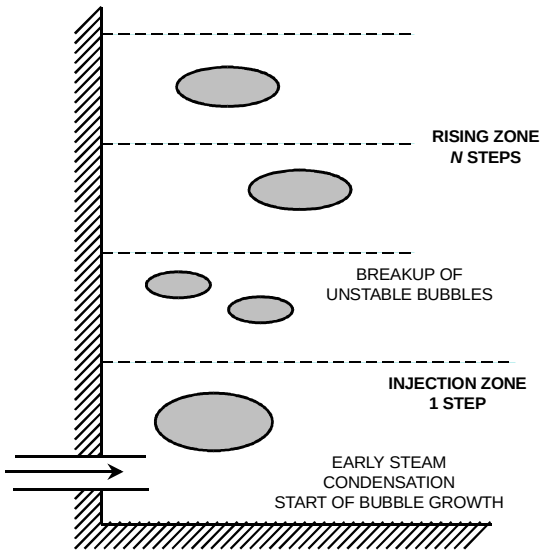

Figure 2.5: ECART bubble rising model.

The aerosol removal efficiency due to the pool scrubbing can be expressed in terms of a

decontamination factor F_D (defined as the ratio of the aerosol mass entering to that escaping from the pool). For each particle size bin, F_D (Figure 2.6) is given as the product of all the decontamination factors associated with the four different aerosol removal mechanisms schematized occurring inside bubbles (never less than unity):

$$F_D = F_{D,co} \cdot F_{D,st} \cdot F_{D,ce} \cdot F_{D,di}$$

$F_{D,co}$ due to steam condensation (diffusiophoresis);

$F_{D,st}$ due to gravitational settling;

$F_{D,ce}$ due to centrifugal deposition;

$F_{D,di}$ due to diffusional deposition.

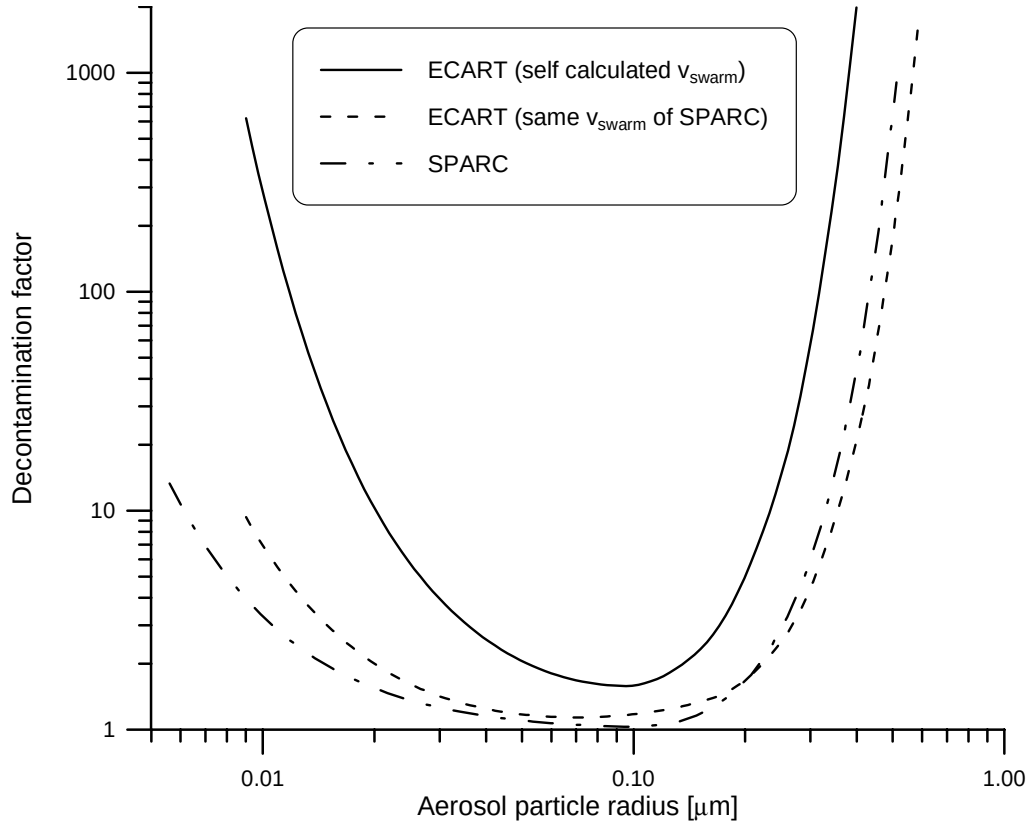

Figure 2.6: Comparison between ECART and SPARC (saturated pool, 50% non-condensable).

The usual well-mixed hypothesis for the aerosol transported inside bubbles is adopted, together with the assumption that the carrier mixture is constantly saturated with steam and in thermal equilibrium with the liquid phase. Evaporation due to depressurization of rising bubbles is not dependent on steam diffusion, but only on thermal-hydraulic boundary conditions (temperature and depth of the pool).

2.1.2.1.1 Bubble History

Even though the carrier gas is injected at a constant flow rate, large globules are formed periodically at the pool entrance. The formation, growth and detachment of these globules have been studied by several researchers. In order to simulate the initial globule formation, ECART adopts a criterion based on experimental observations performed at Battelle Columbus Lab. and other organizations, strongly dependent on the injector diameter and gas velocity, but only very weakly dependent on the injector orientation [Oehlberg 1985].

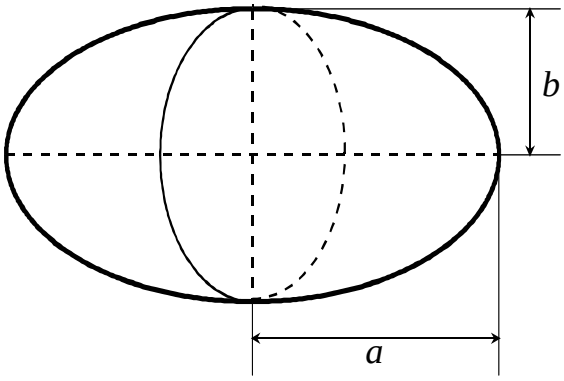

Figure 2.7: Geometrical shape of a bubble.

Bubbles are assumed to have the geometrical shape of an oblate spheroid, i.e., an ellipsoid of revolution along its major axis (Figure 2.7)

The bubble stability is verified by checking the bubble Weber number. According to experimental observations performed at Battelle Columbus Lab., bubbles having a Weber number larger than 15. are considered unstable. Their break-up is simulated in ECART by dividing the bubble into a pair of twin bubbles, until the reduced bubble reaches the stability.

The relative velocity between the bubble and the liquid is calculated using an empirical correlation, like that adopted inside the SPARC code [SPARC 1988a], in good agreement with experimental data presented in the literature.

A swarm of bubbles pumps liquid from the bottom of the pool to the surface and creates a recirculation of the whole liquid phase. The local liquid velocity inside the bubble column, then, increases the bubble rise velocity. An empirical correlation, deduced by Battelle experimental data [Oehlberg 1985], is adopted to roughly calculate a mean swarm velocity as a function of non condensed gas-flow rate.

2.1.2.1.2 Removal Mechanisms Computation

$F_{D,co}$ The steam condensation, if any, is expected only near the injection point (and then within the first rising step: this assumption of thermal equilibrium permits several simplifications, such as to consider the fraction of deposited aerosol equal to the fraction of steam condensed (diffusiophoresis concentrated only in the first rising step) [Owczarski 1983].

The relationship among the mole fractions x_i and x_o of the non condensable gas, respectively before and after the steam condensation, and the volume fraction of the condensed inlet gas f is $\frac{x_i}{x_o} = \frac{1}{1-f}$. The previous assumption implies that this ratio, which is inversely proportional to the bubble volume variation, can be used as a decontamination factor $F_{D,co}$ **associated with steam condensation**, applicable to all the particle sizes. Because the mole fraction of non condensable gases inside the bubble at equilibrium depends on the steam saturation pressure p_w at the pool temperature, and on the total pressure p at the pool inlet, $x_o = 1 - \frac{p_w}{p}$ it turns out to be $F_{D,co} = \frac{1-\frac{p_w}{p}}{x_i}$. Values of $F_{D,co}$ less than unity would mean steam evaporation, with consequent inhibition of particle motion toward interface (in this case, $F_{D,co} = 1$ is imposed): this condition can be reached, for example, if the aerosol enters the pool suspended in a pure non condensable gas mixture. In accordance with its definition, $F_{D,co}$ is modeled in the first axial step only, while the decontamination factors associated with the other mechanisms are modeled at every axial step.

$F_{D,st}$ Being v_s the usual settling velocity [m/s] for a given particle size (accounting for size-dependent shape factors, multicomponent particle density and non-Stokesian behaviour), the $F_{D,st}$ **associated with sedimentation** is calculated from [Owczarski 1983, Alleman 1985, SPARC 1988b]:

$$F_{D,st} = \left\{ \left[\frac{3}{2}(v_s - v) \cdot \left(\frac{a_m}{b_m} \right)^{\frac{2}{3}} \cdot d_m^{-1} \right] \cdot \Delta t \right\}$$

$F_{D,ce}$ **The centrifugal deposition**, caused by the gas recirculation inside the bubble under the friction of the liquid phase, **leads to the decontamination factor $F_{D,ce}$** [Owczarski 1983, Alleman 1985,SPARC 1988b]:

$$F_{D,ce} = \left\{ \left[\frac{6 A_m}{\pi d_m^3} \cdot \left(y^* \cdot v_c - v_v \right) \right] \cdot \Delta t \right\}$$

where v_c is the drift velocity [m/s] due to the centrifugal force and y^* is a corrective factor for non-spherical bubbles, given by [Owczarski 1983, SPARC 1988b].

$F_{D,di}$ Finally, **the diffusional deposition is accounted for by $F_{D,di}$** [Owczarski 1983, SPARC 1988b]:

$$F_{D,di} = \exp\left\{ \left[\frac{6 A_m}{\pi d_m^3} \cdot v_d \cdot \theta \right] \cdot \Delta t \right\}$$

where v_d is the mass transfer coefficient, accounting for the particle thermal diffusivity D_p (dependent on the aerodynamic shape factor χ), and θ is the correction factor described in [SPARC 1988b].

2.1.3 Chemistry Models

The **ch** section provides the **av** section with the gaseous phase composition on the basis of equilibrium conditions. The chemical equilibrium calculation occurs whenever significant changes in temperatures, pressures or vapour species amount are calculated by the other two sections. Possible phase changes causing condensation onto walls and airborne particles, however, are dynamically accounted for in the diffusive model employed by the **av** section.

The solving algorithm is based on Gibbs free energy minimization at constant pressure and temperature of the system: this allows the calculation of the equilibrium composition of the mixture in terms of molar fractions. In order to manage the formation and evolution of radionuclide species within LWR Reactor Coolant Systems, this **ch** section is dimensioned for environments characterized by temperatures in the range from room conditions up to 2,500. K, with pressures up to 15. MPa. Real gas behaviour is modelled by fugacity coefficients computed according to Redlich-Kwong-Soave equation for a hydrogen-steam mixture. The code uses a non-linear minimization

algorithm preventing the linearization of the function to be minimized, which would affect the correctness of final results.

The possible reactants and reaction products considered (Table 2.1) are the carrier gas components, with the exception of nitrogen and noble gases, and most of the species which can be transported in form of vapours. To match with the phase changes calculated by the **av** section, super saturation conditions of the predicted vapours are accepted by chemistry algorithms. The databases contained in chemical section are also used to determine the temperature-dependent saturation pressures of all volatile species. The **ch** section contains information about the most representative compounds for a LWR SA sequence. Further compounds, involved in fusion reactor safety problems, are also included in the catalogue (Table 2.1) as discussed in the next paragraph.

2.2 Models for Chemical Reactions in Fusion Reactor Accidents

ECART allows fitting the fusion reactors model for the oxidation reactions of beryllium, graphite and tungsten in air and steam. These reactions involve three features modelled by the code: heat structures, aerosol particles suspended in the carrier gas and aerosol particles deposited on walls.

The reactions of beryllium, graphite and tungsten solid walls of PFCs or dusts with air and/or steam are not explicitly treated by the chemical section of ECART but in a separate ad-hoc module which makes use of surface reactions rates computed by means of semi-empirical correlations, also giving the reaction heats released to or removed from the environment. The oxidation reactions are only limited by the availability of steam and oxygen in the carrier gas, while the mass of the reacting element (Be, C or W) in the suspended or deposited aerosol cannot become negative (on a solid wall, the reacted elements Be, C and W and the solid oxide reaction products BeO and WO_3 are not accounted for).

If the amount of steam or oxygen required by all the reactions occurring concurrently, in the current time step, is greater than the available mass, the Δm of each reaction is scaled by the ratio of the available to the required mass of steam or oxygen. In this way, no reaction is favoured but some delay in the reaction completion could result.

Obviously, in a stand-alone aerosol-vapour analysis, no account is taken of the reaction heating and of the mass addition to or subtraction from the carrier gas because the thermal-hydraulic conditions are fixed by input tables. On the contrary, for the reactions occurring in the suspended or deposited aerosol, the mass increase (or decrease) in a time step or sub-step, of the involved chemical species

(e.g., Be and BeO) is allowed for in the mass balance equations and is distributed over the aerosol size bins proportionally to the square of the geometric mean radius of the particles.

If a thermal-hydraulics/aerosol-vapour coupled analysis is performed, the reaction heat (positive for exothermic reaction) is added to the gas atmosphere for reactions occurring in the suspended aerosol and is added to the structure for reactions occurring on the solid surface or in the deposited aerosol.

The masses of the carrier gas components (steam, hydrogen, oxygen, carbon monoxide and dioxide) released or removed by the reactions, as well as the correspondent enthalpies, are accounted for in thermal-hydraulics.

The reactions in the suspended aerosol are assumed to occur at the gas bulk temperature, while the boundary layer temperature (i.e. geometric mean of wall and gas bulk temperatures) is used for the reactions with solid walls and deposited aerosols. This last assumption is questionable and it is under further assessment.

The reaction area is identified with the wall surface area for the reactions on a solid wall and with the surface area of all the particles multiplied by the mass fraction of the reacted element for the reactions in the airborne aerosol. Also, as far as the reaction area for the deposited aerosol is concerned, the total surface area of the aerosol particles is assumed except when the deposited liquid mass exceeds a given fraction of the total deposited mass, in which case the area of the underlying wall is assumed. However, for a multi-layer deposited aerosol, the basic reaction area should be reduced depending on the depth of the deposited aerosol and on the dispersion (standard deviation) of the aerosol particles distribution, i.e., on the compactness of the aerosol agglomerate.

Table 2.1: Catalogue of the chemical species available in ECART.

Species Name	Species Description	Normal melting point [K]	Normal boiling Point [K]	Solid density [kg/m^3]	Liquid density [kg/m^3]	Evaporat. / Condens.	Chemi-sorption
Ag	Silver	1234.	2436.	10500	9320	Yes	No
AgI	silver iodide	831.	1779.	5683	4830	Yes	No
B	Boron	2350.	4139	2355	2080	Yes	No
BI3	boron triiodide	323	483	3350	3350	No	No
B2O3	boron sesquioxide	723.	2133.	2460	2090	Yes	No
Ba	Barium	1000.	2119.	3510	3081	Yes	No
BaI	Barium monoiodide	--	--	--	--	No	No
BaI2	Barium iodide	984.	2337.	5150	4380	Yes	No
BaO	Barium oxide	2286.	--	5720	4862	Yes	No
BaOH	Barium hydroxide	--	--	--	--	No	No
Ba(OH)2	Barium dihydroxide	681.	1325.	2180	1850	Yes	No
Be	Beryllium	1560.	2741.	1850	1500	Yes	No(3)
BeO	Beryllium oxide	2821.	--	3010	2258	no	No(3)
C	Carbon	3925.	5100.	2250	1912	no	No(3)
Cd	cadmium	594.	1038.	8642	7530	yes	No
CdI	cadmium monoiodide	--	--	--	--	no	No
CdI2	cadmium diiodide	660.	1069.	5670	4820	yes	No
CdO	cadmium oxide	--	--	6950	5900	yes	No
Cd(OH)2	cadmium dihydroxide	--	--	4790	4070	no	No
CdTe	cadmium telluride	1314.	--	6200	5270	no	No
CH4	methane	--	--	--	--	no	No
Co	cobalt	1768.	3198.	8900	7670	yes	No
Cr	chromium	2130.	2945.	7200	6460	yes	No
CrI	chromium monoiodide	--	--	--	--	no	No
CrI2	chromium diiodide	1129.	--	5196	4417	yes	No
CrO	chromium oxide	--	--	--	--	no	No
Cr2O3	chromium sesquioxide	2603.	4273.	5210	4430	no	No
Cs	Caesium	301.5	948.	1878	1468	yes	No
CsBO2	Caesium borate	--	--	--	--	no	No
CsI	Caesium iodide	900.	1553.	4510	4057	yes	No
CsO	Caesium monoxide	--	--	--	--	no	No
CsOH	Caesium hydroxide	500.	1263.	3675	3308	yes	sorbable(1)
Cs2	diatomic caesium	--	--	--	--	no	No
Cs2CrO4	Caesium chromate	--	--	4237	4237	no	No
Cs2MoO4	Caesium molybdate	-	-	1000	0850	yes	No
Cs2O	Caesium oxide	763.	763.	4250	3610	yes	No
Cs2(OH)2	Caesium dihydroxide	--	--	--	--	no	No
Cs2Te	Caesium telluride	--	--	--	--	no	No
Cs2TeO3	Caesium tellurite	--	--	1000	0850	no	No
Cs2ZrO3	Caesium zirconate	--	--	1000	0850	no	No
Cu	copper	1358	2843	8920	7950	yes	No

CuO	Copper monoxide	1599	2073	6400	5440	yes	No
D	Elemental deuterium	--	--	--	--	no	No
D2	molecular deuterium	--	--	--	--	no	No
Fe	Iron	1809.	3132.	7860	7020	Yes	sorber(2)
FeI2	iron iodide	-	-	5320	4522	yes	No
FeO	iron oxide	1650.	3687.	5700	4840	yes	No
Fe2I4	iron iodide	--	--	--	--	no	No
Fe2NiO4	diiron nickel tetraoxide	--	--	--	--	no	No
Fe2O3	iron sesquioxide	1838.	--	5240	4450	no	No
Fe3O4	iron tetraoxide	1870.	1870.	5180	4400	no	No
H	elemental hydrogen	--	--	--	--	no	No
HBO2	boric acid	--	--	--	--	no	No
HI	hydrogen iodide	--	--	--	--	no	Yes
H2O	water	273.	373.	1000	1000	yes	No
H2Te	hydrogen telluride	--	--	--	--	no	No
H3BO3	boric acid	--	--	--	--	no	No
I	elemental iodine	--	--	--	--	no	Sorbable
I2	molecular iodine	387.	458.	4930	4930	yes	Sorbable
In	indium	430.	2353.	7300	5585	yes	No
InI	indium monoiodide	624	986	5310	4514	yes	No
InTe	indium telluride	342.	--	6290	6290	no	No
In2O	indium suboxide	--	--	6990	6990	no	No
In2O3	indium sesquioxide	--	--	7179	6100	no	No
In2Te	diindium telluride	--	--	--	--	no	No
Li2O	Lithium oxide	1843.	2836	2013	1711	yes	No
LiOH	Lithium hydroxide	744.	1897	1460	1241	yes	No
Mn	manganese	1517.	2332	7200	6430	Yes	No
MnI2	manganese diiodide	911.	--	5000	4250	No	No
MnO	manganese oxide	2115.	--	5445	4630	No	No
Mn2O3	manganese sesquioxide	--	--	4500	3820	No	No
Mn3O4	trimanganese tetraoxide	1835.	1835.	4856	4130	No	No
MoO2	molybdenum dioxide	--	--	6470	5500	Yes	No
MoO3	molybdenum trioxide	1075	1428	4692	3988	Yes	No
Ni	nickel	1726	3005.	8900	7780	Yes	Sorber(2)
Ni(CO)4	nickel carbonyl	248	316	1320	1320	No	No
NiI2	nickel iodide	1070.	--	5834	4960	No	No
NiO	nickel monoxide	2263	--	6670	5700	Yes	No
O	elemental oxygen	--	--	--	--	No	No
OH	hydroxyl	--	--	--	--	No	No
RbI	rubidium iodide	929.00	--	3550	2870	Yes	No
RbOH	rubidium hydroxide	574.	--	3203	2723	No	No
Ru	ruthenium	2523.	4173.	12300	10900	Yes	No
RuO2	ruthenium dioxide	--	--	6970	5920	No	No
RuO3	ruthenium trioxide	--	--	--	--	No	No
Sb	antimony	904.	2023.	6684	5681	Yes	No

SbTe	antimony monotelluride	--	--	--	--	No	No
Sb2	diatomic antimony	--	--	-	-	no	No
Sb2O3	antimony trioxide	939.	1823.	5670	4820	no	No
Sb2Te3	antimony tritelluride	902.	--	6500	5525	no	No
Sb4	tetraatomic antimony	--	--	--	--	no	No
Sn	tin	505.	2873.	7280	7000	yes	No
SnH4	tin tetrahydride	--	--	--	--	no	No
SnI2	tin iodide	593.	990.	5290	4497	yes	No
SnO	tin monoxide	--	--	6446	5448	yes	No
SnO2	tin dioxide	1400.	2073.	6950	5910	no	No
SnTe	tin monotelluride	1079.	--	6480	5510	yes	No
Sr	strontium	1050.	1685.	2600	2210	yes	No
SrI2	strontium iodide	811.	2178.	4549	3870	yes	No
SrO	strontium oxide	2938.	3273.	4700	3990	no	No
SrOH	strontium hydroxide	--	--	--	--	no	No
Sr(OH)2	strontium dihydroxide	783.	1017	3625	3080	yes	No
T	Elemental tritium	--	--	--	--	no	No
T2	molecular tritium	--	--	--	--	no	No
Te	Tellurium	723.	1327.	6250	5489	yes	sorbable(1)
TeO2	tellurium dioxide	1006.	1518.	5790	4920	yes	No
Te2	diatomic tellurium	--	--	--	--	no	sorbable(1)
W	Tungsten	3680.	5931	19350	17600	yes	No(3)
WO3	Tungsten trioxide	1745.	2110	7160	6086	yes	No(3)
Zn	Zinc	693.	1179.	7140	6570	yes	No
ZnO	zinc oxide	2248.	--	5606	4770	no	No
ZrI4	Zirconium tetraiodide	772.	--	1000	1000	yes	No
ZrO2	zirconium dioxide	2950.	4544.	5890	5010	yes	No
&...	inert species(4)	Input	--	input	Input	no	No

(1) *Also chemisorbable on steel wall and aerosol particles if Fe and/or Ni are present*
(2) *Also sorber for chemisorption in aerosol particles*
(3) *Involved in oxidation reactions with steam and oxygen*
(4) *Inert as aerosol, not requiring chemical equilibrium or phase change calculation, input added by user*

3. CHARACTERISTICS OF THE ANALYSIS

The description of the present LOFA + in-vessel LOCA scenario, including the main numerical values of the different input parameters to be assumed in the analysis are taken from the ENEA Fusion Division Report FUS-TN-SA-SE-R-47, *"Accident Description for Power Plant Conceptual Study"*, Rev. 1, [Di Pace, 2002].

3.1 Description of the Accident Scenario

The postulated accident is a pump trip in one of the FW/BL HTS leading to a loss of flow in one of the cooling loops, without pump coast-down (see Figure 3.1). The FPSS does not intervene. The PFCs increase their surface temperatures until 1,073 K (average temperature over 4 mm for the FW EUROFER material between cooling channel and plasma) are reached [Hermsmeyer, 2002] and a break in the in-vessel FW/BL cooling channels happens, with a reference cross section equal to 7.36e-4 m^2 (corresponding to 2 cooling channels, average dimensions 0.023 x 0.016 m).

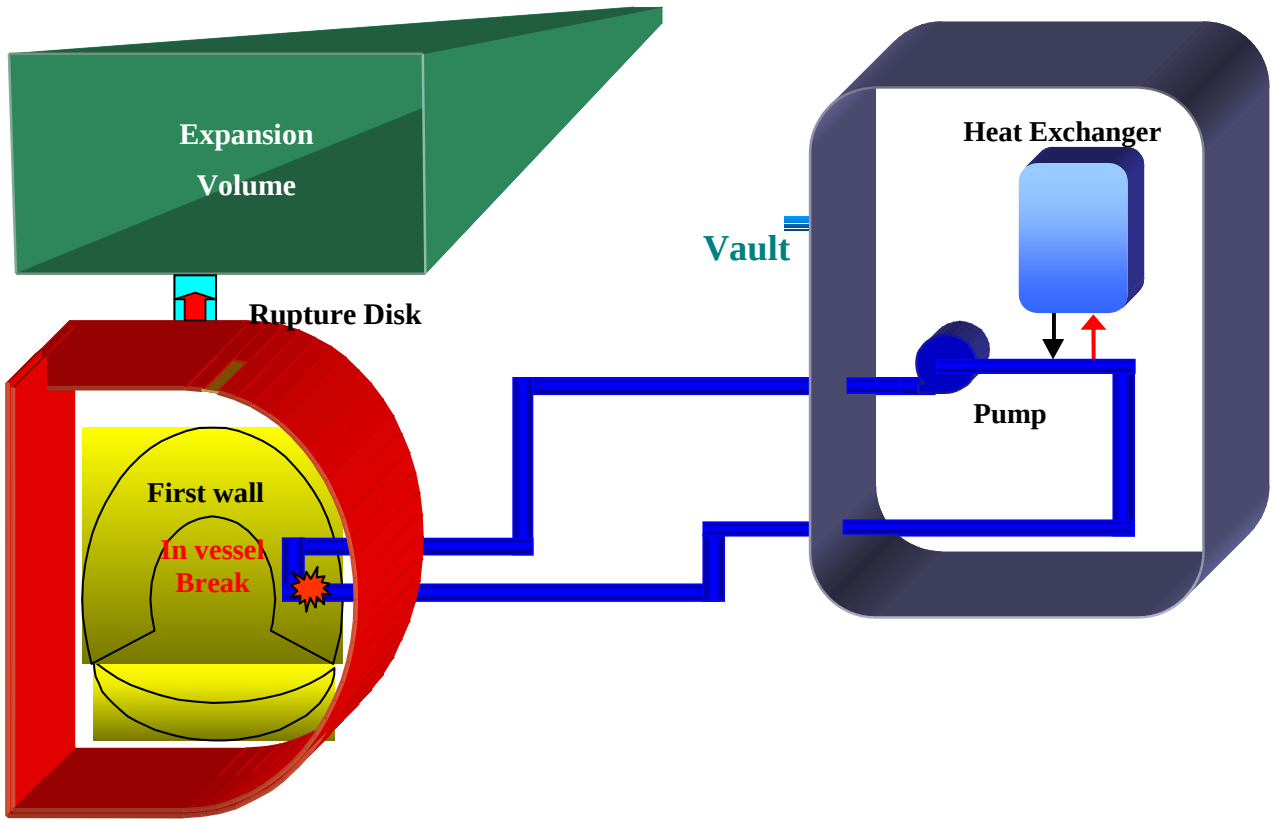

Figure 3.1: Sketch of the LOFA + in-vessel break accident.

All the control systems (relief valves and pressurizer) in the cooling loops will be excluded at the beginning of the accident. A plasma disruption occurs, having an energy deposition of 6.0 MJ/m^2 hitting an area of 418.0 m^2 in the FW zone for 1.0 s. The FW/BL of the failed loop is first cooled down with residual coolant present before the complete drainage.

In this transient the VV atmosphere is supposed to be an initial temperature equal to 200 °C. When the VV total pressure reaches 0.10 MPa a rupture disk (in the PPCS design with a tentative size 2.0 m^2)[2] opens toward the EV, having a tentative free volume of 68.000 m^3 (initial conditions of the air internal atmosphere 30.0 °C and 0.09 MPa) [Di Pace, 2002].

Leakages from the VV and EV building towards the external environment has been initially considered as specified in the following Table 3.1. The first ECART simulations [Paci, 2003] highlighted **the too high value of the specified EV daily leak rate (75%)**. This value implies too high releases of radioactive materials at 24 hours from the beginning of the sequence, especially for the tritium gas, also if the EV total pressure remains well under the design one. So, a series of parametrical runs was carried out [Paci, 2003], varying this value of the daily leakage rate (1%, 10% and 75% of volume/day) and showing the strong influence of this design parameter. This results have been confirmed also in the present analysis, where two values (1% and 75% of the free volume) for the maximum EV daily leakage have been considered.

	Design pressure P_D (MPa)	**Leak rate (% volume/day)**	**Scale rules leakage [m^3/s]**
VV	0.2	5 % (at design pressure)	Scales with square root of differential pressure $\text{leakage} = \frac{0.05 \cdot \text{Volume}}{24 \cdot 3600} \sqrt{\frac{P - P_0}{P_D - P_0}}$
EV	0.16	75 % (at design pressure)	Scales with square root of differential pressure $\text{leakage} = \frac{0.75 \cdot \text{Volume}}{24 \cdot 3600} \sqrt{\frac{P - P_0}{P_D - P_0}}$

P current pressure P_0 atmospheric pressure 24 = hours per day 3600 = seconds per hour

Table 3.1: Leakages laws for VV and EV.

[2] This size of 2.0 m^2 is too large for the reference scenario (but it is also true for a stronger transient with a break area increase of a factor 10.) and in the reference analysis [Paci, 2003] the rupture disk area was reduced to 0.2 m^2.

For the assumption of the radioactive materials inventories and their mobilization see Table 3.2. This table is built [Di Pace, 2002] on the basis of the SEAFP values for the tritium present inside the VV and the amount of dusts. The dusts granulometry assumed in the ECART analysis and reported in Table 3.2, are based on [Honda, 2000]. For the SS dust and W dust no granulometry differences have been assumed, so no multicomponent analysis are necessary and the released fractions, respect to the initial mass inventory, are the same for the two kinds of dusts (the aerosol particles behaviour is the same manner for the two species).

Source terms	Model B	Notes
Tritium in VV	1 kg	Initially present in VV
SS Dust	7.6 kg	AMMD 1.2 micron GSD 2.0
W Dust	2.4 kg	AMMD 1.2 micron GSD 2.0
Tritium in coolant	1.0 g (per loop)	Released into VV
ACPs total inventory	0.0 g	
Sputtering products	0.0 g	

Table 3.2: Tritium and dusts inventories.

A transient of 24 hours has to be analysed, taking into account the decay heat in the in-vessel structures, with an initial nuclear heating of 1.85 MW/m^2 [Porfiri, 2002], on the basis of the Athena results for the helium release and the PFC surface temperatures [Meloni, 2003]. In particular, it has been assumed that the cooling goes on in the not affected loops and it has been taken into account the heat conduction from the FW/BL structure towards the VV. Other information on PFC structures, including the decay heat time history and surfaces, has been communicated by ENEA Fusion Division [Porfiri, 2002].

The scope of the first ECART analysis [Paci, 2003] was to optimise the dimensions of the EV and RD, in order to avoid too high peaks of total pressure impairing the containments (VV and EV). The final goal was to demonstrate that the overpressure in the VV is safely mitigated under the design pressure of 0.2 MPa. From those analyses a first indication about the external releases and their mitigation was also derived, starting the further analysed presented in this report.

3.1.1 The Confinement Option for Model B

The confinement option described in the following is applicable only for the PPCS Model B (Helium cooled). The model B confinement includes an expansion volume EV, whose volume size has to be sufficient to accommodate the total release of gas without peaks above the design pressure. The EV will be also used to relief the pressure both in the VV and in the cooling system room. The main parameters of this confinement option are reported in Table 3.3:

VV design pressure	0.2 MPa
2nd containment design pressure	0.16 MPa
Disk rupture opening set point pressure from VV to EV	0.10 MPa
Area of the disk rupture from VV to Expansion Volume	2.0 m^2
Area of the disk rupture from VV to EV assumed in ECART analysis	*0.2 m^2*

Table 3.3: Main parameters of the confinement option.

3.2 Plant Nodalisation and Analysis Specifications

A PPCS nodalisation, not including a direct simulation of the helium release into VV, as present in integrated analysis [Paci, 2003], but on the contrary using an external superimposed blow-down table obtained by the Athena code [Meloni, 2002], was set up at DIMNP for ECART in order to permit a fast and reliable assessment of different parametrical conditions for this sequence, according to the specifications for this accident sequence analysis [Di Pace, 2002].

All the main data required to the PPCS description (geometry, materials, initial thermal-hydraulics conditions, etc.) are taken from these references, while the specifications of the new parametrical analysis have been set-up in a meeting at the ENEA Frascati Lab between ENEA Researchers and Pisa University ones [ENEA, 2003].

The main points to be analysed in the present report, mainly quantifying their influence on the PPCS Model B external radioactive releases of tritium and dusts, and highlighted in the previous mentioned meeting, are the following ones:

- presence of a detritiatiation system (DS) for the EV, having a constant mass flow-rate of 3.0 kg/s and a removal efficiency of 99.9% both for tritium and dusts;

- maximum daily leakage rates of the EV (two values: 1% and 75%, with the pressure dependence specified in Table 3.1);
- presence of a dust scrubber, after the rupture disk (RD) between the VV and the EV, having an imposed DF, fixed equal to 0.9;
- fraction of the initial dusts mass resuspended inside the VV at the beginning of the sequence (two values: 100% and 50% of resuspended mass).

Starting from these 4 points, the 16 parametrical analysis reported in Table 3.4 have been identified during [ENEA, 2003]. In the same table also the identifying tag of each run is reported. For each of these 16 parametrical analysis the total quantity of tritium gas, SS and W dusts released to the external environment, including the subdivision for the release pathway, have been evaluated using ECART.

	EDS	lkg	Scrub	risosp		EDS	lkg	Scrub	risosp
reference	no	75%	no	100%	6	3.0	75%	no	100%
1		1			7		1		
2		75		50	8		75		50
3			yes	100	9			yes	100
3r				50	9r				50
4		1		100	10		1		100
4r				50	10r				50
5			no	50	11			no	50

Table 3.4: Parametrical analyses performed.

The main nodalisation problem was the analysis of the dust scrubber having an imposed and fixed DF. Normally, this DF is automatically calculated by the code itself for a water scrubber, as described in the previous Paragraph 2.1.2.1, as a function of the water scrubber characteristics (pool deep, orifice diameter, orifice number, etc.) but, at the present stage of the PCCS design, these characteristics were not available. So, it was decided [Porfiri, 2003] to use a fixed value for the DF equal to 0.9, as indicated in some reference documents on this phenomenology [NEA, 2000], [Boerrigter, 2002]. But, inside the ECART input options, it is not possible to specify a fixed value of the DF at a specific junction.

To override this code input limitation, the following methodology has been adopted for all the scrubber analyses:

a) a first ECART nodalisation (Figure 3.2) has been developed, without the presence of the scrubber at the RD junction (obviously this nodalisation has been employed also for the parametrical runs without the scrubber presence). The nodalisation implies 6 control volumes (2 regular nodes – VV and EV - and 4 back environments), 4 heat structures (three EUROFER for VV and 1 concrete for EV, not specified inside [Di Pace, 2002] but analysed[3] in [Paci, 2003]), no implicit junction and 6 explicit junctions, 5 depending on time or pressure, including the RD, plus the explicit junction, with imposed mass-flow, simulating the helium release into the VV. Four non-condensable gases (N_2, O_2, He and CO_2) have been accounted for in thermal-hydraulic module plus the T_2 gas considered inside the aerosol module, together with SS and W dusts resuspended inside the VV.

b) Utilising this nodalisation, the time dependent mass flows of tritium, SS and W in the RD junction has been evaluated without DF calculation for the scrubber pool (the scrubber is simulated as an 1-m height sump on the bottom of the EV, where the exit of the RD junction is submerged);

c) A DF equal to 0.9 has been separately applied, using Microsoft Excel©, to the SS and W mass flows, calculating the reduced mass flow rates for these two species entering into the EV. This DF has been applied for all the code aerosol bins, loosing the dependence of the scrubbing action on the particles size (Figure 2.6). The granulometry of these dusts (AMMD and GSD) has been assumed equal to the one calculated during the phase a) for the particles suspended inside the EV.

d) A second nodalisation has been employed, very similar to the previous one, but with the reduced mass flows of SS and W directly injected inside the EV atmosphere, using two new time dependent tables not present in the phase a) while the tritium gas, not influenced by the scrubber DF, is always injected inside the VV atmosphere. With this second nodalisation the gas and dust external releases from the EV have been evaluated, while the releases from the VV are the ones calculated during the phase a). This assumption was possible because the presence of the scrubber pool avoids, in the long term of the sequence, back flows of dust and gases from the EV to VV, for pressure differences less than 0.01 MPa (these back flows

[3] The total concrete surface has been fixed equal to 9,246.412 m^2, equivalent to a cylinder with a free volume of 68,000.0 m^3 and 40.0 m height.

on the contrary possible when only the RD is present). So, with the pool scrubber presence, when tritium or dusts are transported into the EV it is no more possible their external release from the VV leakage and the two release paths, present in the PPCS design, can be analysed in a separate way.

e) Finally, the two releases quantities (from VV and from EV) are added for the global evaluation of the PPCS external releases for the 3 different chemical species. It has to be noted that the separated evaluation of the two release paths (VV and EV) is fundamental for the right understanding of the mechanism of the 3 proposed different mitigation actions (DS, pool scrubber and increase of the EV tightness).

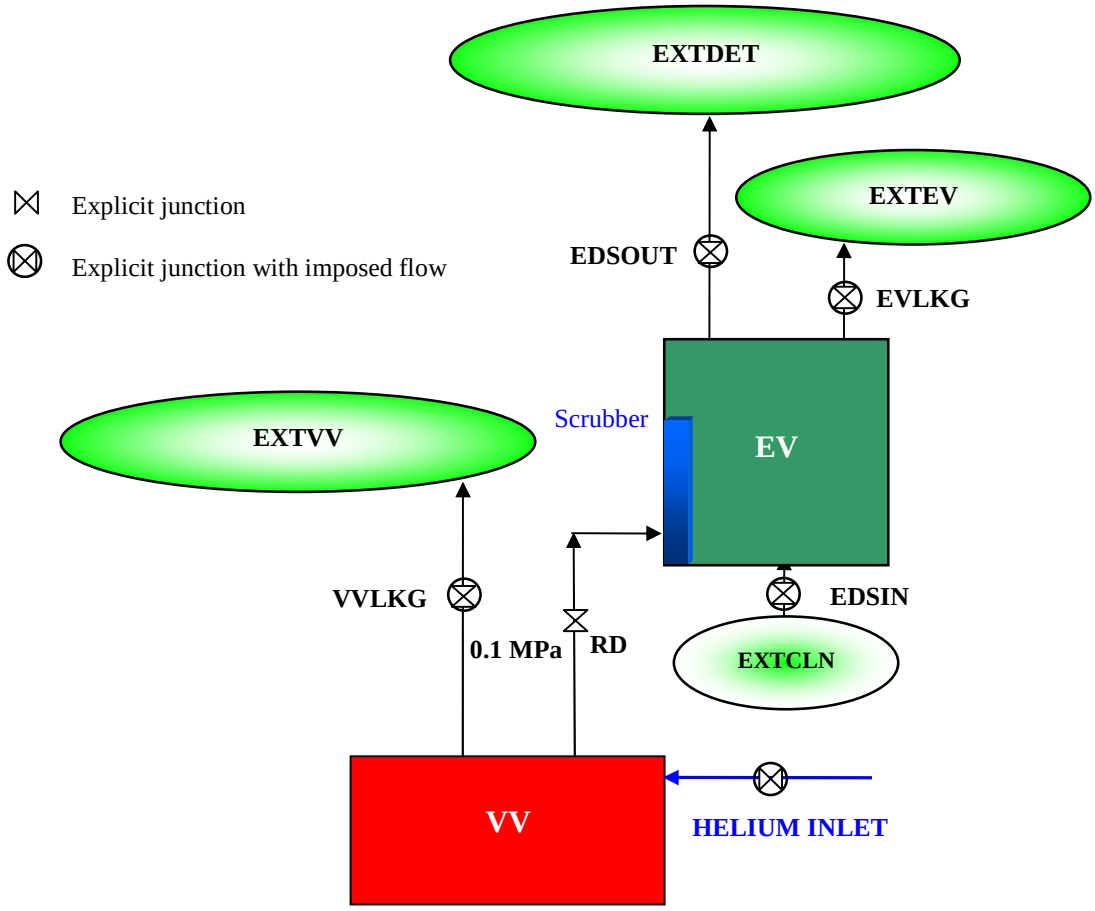

Figure 3.2: General nodalisation adopted for ECART analyses of PPCS.

3.2.1 Further Input Data

Two different types of materials and their temperature-dependent thermal properties (EUROFER and concrete) have been included in the input tables. The appropriate boundary conditions (i.e., time trends of the external temperatures and of the external heat transfer coefficients) have been imposed for the PFC structures (Figure 3.3), to reproduce the disruption thermal loads and the cooling action of the working HTS [Meloni, 2003]:

DV horizontal steel structure having a surface area of 391.0 m^2, facing with the VV and cooled on outside at 673. K, located on the VV bottom. Only one region is present, the 0.01 m thickness surface region facing the VV, with 4 thermal meshes.

FW vertical steel structure having a surface area of 1,253.0 m^2, facing with VV and HTS, uniformly distributed inside the VV. Two regions are modelled, with different mesh sizes: the 0.01 m thickness surface region, facing the VV, with 4 thermal meshes and the internal region of 0.57 m thickness with 28 meshes. In the surface region the decay power is simulated imposing the Athena temperature data [Meloni, 2003].

The coolant flow-rate into the VV atmosphere (HELIUM INLET) is given into the ECART input deck on the basis of the Athena helium mass flow-rate results [Meloni, 2003], reported in Figure 3.4.

The overpressurization of the VV is limited by the presence of the very big Expansion Volume (EV) connected to the VV through a rupture disk (RD), with an opening set point of 0.1 MPa and a discharged flow area reduced at 0.2 m^2, as discussed in [Paci, 2003].

The leakages from the VV due to the node overpressurization are conveyed to an external volume (EXTVV), representing the room hosting the VV itself. The law of the mass flow-rate as a function of VV pressure for this leakage (explicit junction VVLKG), as for the EV leakages, has to be input specified, for the lack in the ECART code of a specific model for this kind of containment leakages (daily percentage of the total free volume at the design pressure). Obviously the leakages from the EV atmosphere into the external environment (now simulated with the EXTEV volume) occurs through another explicit junction (EVLKG).

The presence of the Detritiation System (DS) (once through) for the EV atmosphere was considered with a retention efficiency equal to 99.9% for both tritium and dusts [Honda, 2000]. This DS connects the EV atmosphere with the external environment (EXTDET) through the explicit junction

EDSOUT, with a constant mass flow-rate (3.0 kg/s), again evaluated in [Paci, 2003]. A further back-environment control node, simulating the external clean atmosphere (EXTCLN), has been added into the PPCS nodalisation in order to simulate the 3.0 kg/s clean air ingress (from the explicit junction EDSIN) into the EV atmosphere due to the presence of the DS.

All the PPCS plant parts involved in accident analyses are assumed to possibly discharge the polluted streams into the external environment, but distinguishing both the pathway and the origin (and, of course, the leakages/intake laws). This fundamental result has been obtained by input assigning 3 different "back-environment" discharge volumes in the nodalisation:

- Discharge by leakages from the VV (into EXTVV);
- Discharge by leakages from EV (into EXTEV);
- Discharge from EV through the DS (explicit junction EDSOUT) into EXTDET.

The details of the developed PPCS nodalisation and all the data and code options employed for the present analysis (in-vessel break in the helium coolant loop of FW/BL HTS), including the simulation of the DS and of the pool scrubber, are reported in the ECART input list in the final Appendix, referring to the case 3.

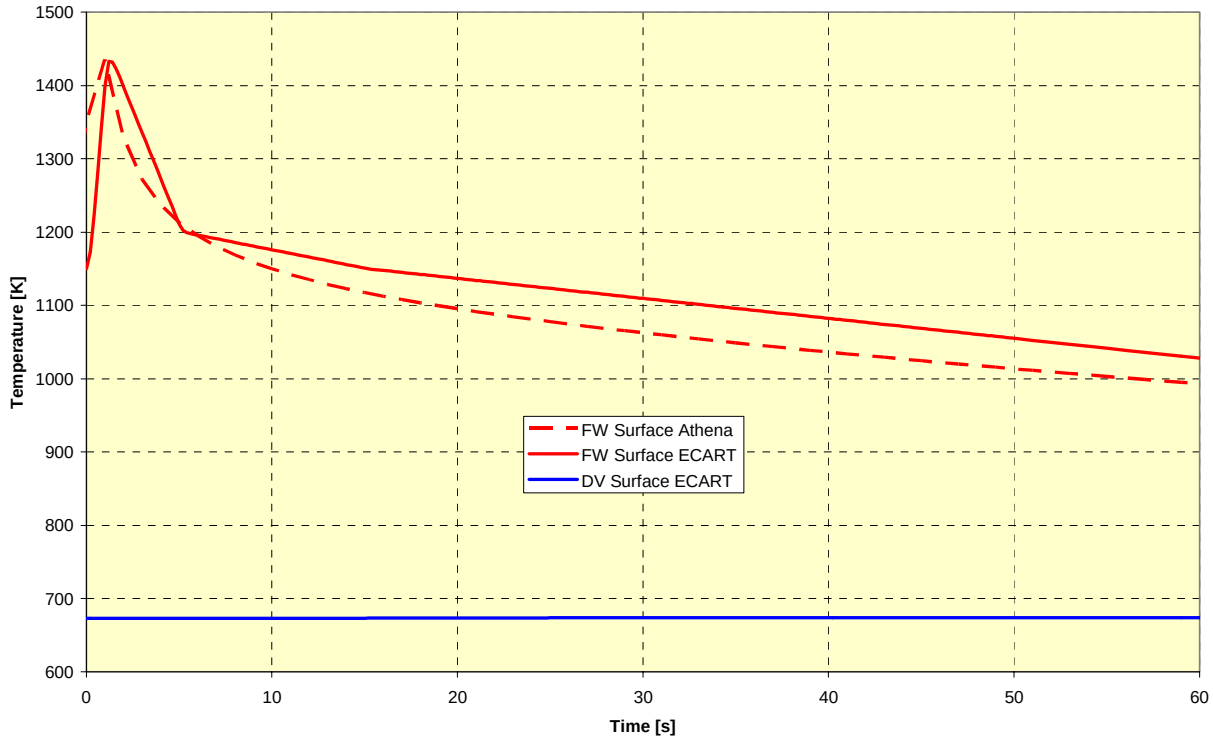

Figure 3.3: FPC structures initial temperature trends (case 0).

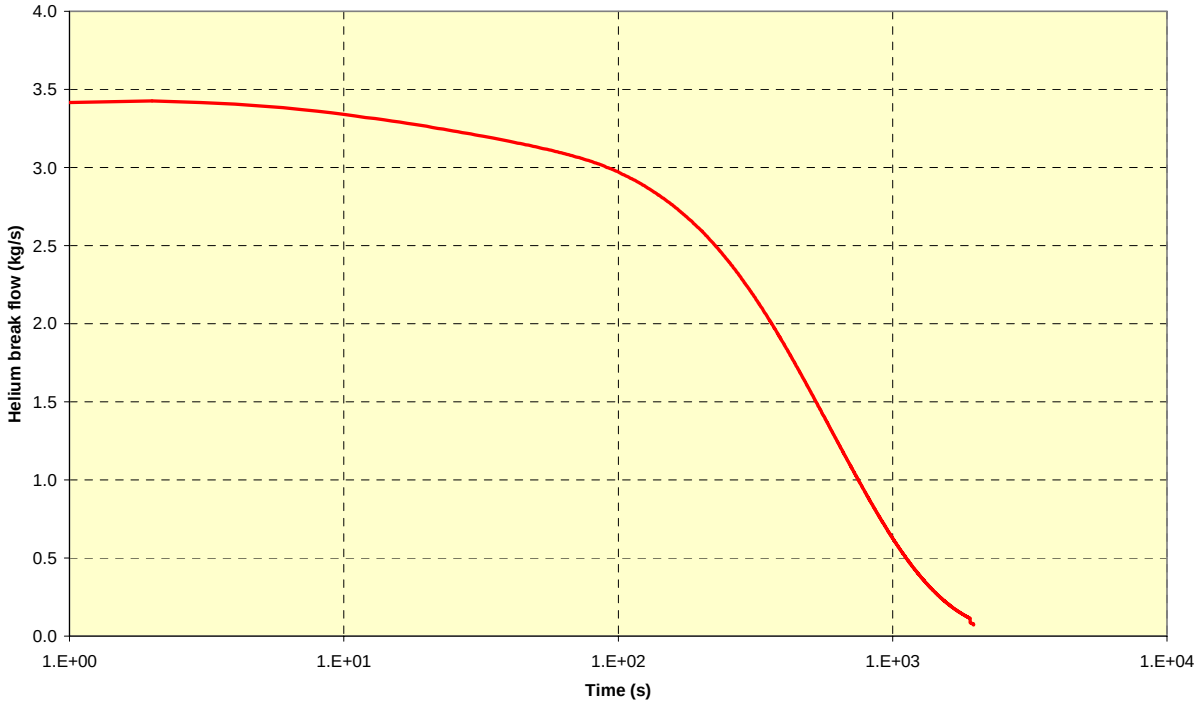

Figure 3.4: Helium coolant blow-down predicted by Athena.

3.2.2 Tritium and Aerosol Initial Inventory

The inventory and the characteristics of tritium and dust involved in the accident (Table 3.2) are taken from [Di Pace, 2002]:

- 1001.0 g of tritium, as $\mathbf{T_2}$ gas, are assumed to be present inside the VV atmosphere at the beginning of the transient ("time zero" is the time of the occurrence of the "in-vessel" break);
- 2.4 kg of tungsten **W** and 7.6 kg of Stainless Steel **SS** are the inventories of dusts inside the VV. According to [ENEA, 2003], all the mass of these dusts (or 50%) is assumed to be suspended inside the VV atmosphere at the beginning of the transient because of the strong initial resuspension forces caused by the inlet of the helium coolant blow-down.

Investigations are under way [Parozzi, 2002], [Porfiri, 2003a] to estimate the realistic mobilisation (i.e. the re-suspension fraction) of the VV dust inventory, also from an experimental point of view.

About the initial granulometry of the different dust particles, the following assumptions have been made, as assumed in [Honda, 2002]:

W & SS Tungsten and Stainless Steel dust particles have the same initial AMMD of 1.2 micron, with a half theoretical density and the same initial geometric standard deviation GSD equal to 2.0 (see Figure 2.4).

All the dust particles are assumed to have a standard spherical shape (the code dynamic shape factors are imposed equal to the defaults values, i.e., $\chi = \gamma = 1.0$). This assumption is questionable for the absence of liquid water inside the VV [Parozzi, 1997b] but it is conservative because hypothetical larger or agglomerated particles will have a higher gravitational deposition velocity and so the possible retention process, in this way, is minimised in the present nodalisations. The asphericity of the dust particles should be simulated by input assigning two different "*dry*" shape factors: the "*aerodynamic shape factor*" χ, accounting for different resistance to motion of the actual particles if compared to the mass-equivalent sphere, and the "*collision shape factor*" γ, accounting for the increased effective collision cross-section. The standard utilised two values for DIMNP analysis of a LWR RCS are $\chi = 2.0$ and $\gamma = 2.0$ (see Figure 3.5) [Brockmann 1985].

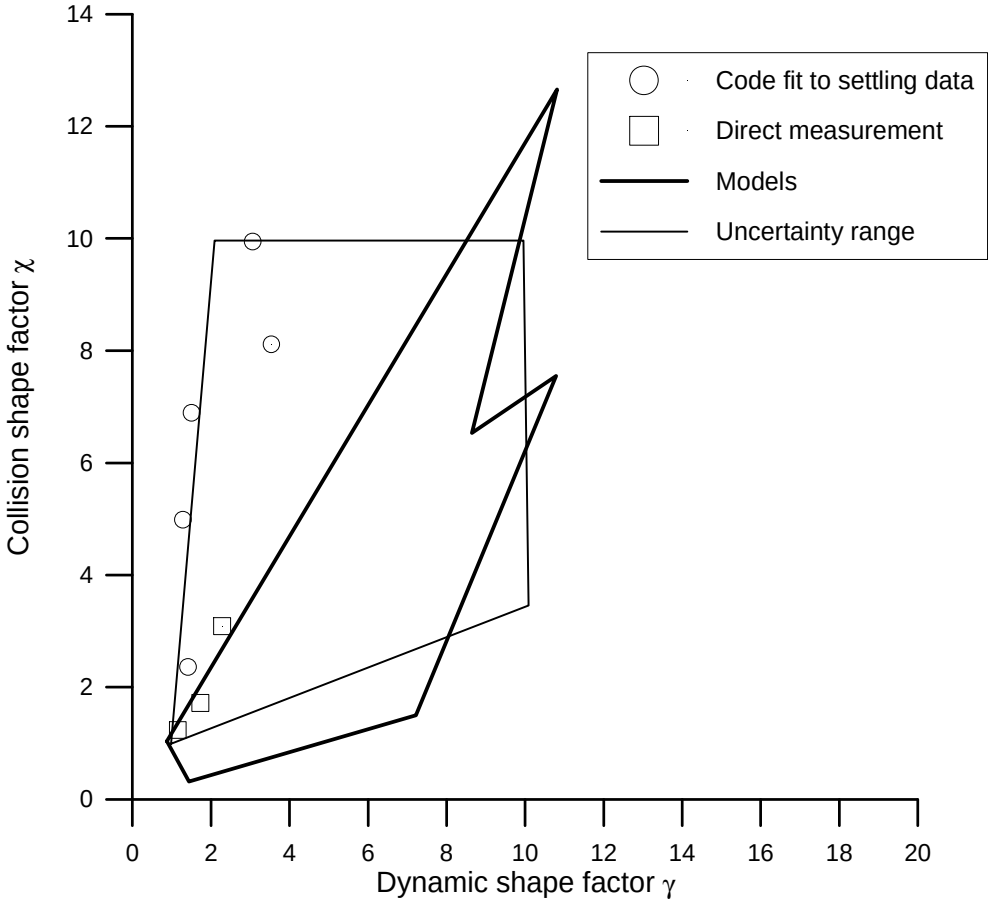

Figure 3.5: Experimental-theoretical shape factor regime for dry aerosols.

4. ECART RESULTS

The results of the previous analysis carried out with ECART [Paci, 2003] state the **capability of the PPCS Model B confinement design to withstand this severe "LOFA + in vessel LOCA" thermal-hydraulic transient, from the design pressure point of view, but the radioactive releases to the external environment are too high for this particular sequence and confinement design characteristics,** especially considering the very low tightness capability of the EV (at a daily leak rate of 75%). For this reason, as previously discussed, the present work on the influence on the external releases of possible mitigation actions has been carried out.

In the reference calculation, also presented in this Chapter 4, on the basis of [ENEA, 2003] and [Paci, 2003], the following PPCS confinement main parameters have been assumed (the deviations from the specifications [Di Pace, 2002] are highlighted in *italic*):

- EV free volume: 68,000 m^3
- Maximum EV leakages: 75% daily
- *One cylindrical (40.0 m high) concrete structure surrounding the EV, initially not specified, having a total internal surface area of 9,246.412 m^2 and a thickness of 0.4 m, externally insulated*
- *Rupture disk RD area: 0.2 m^2 (vs. 2.0 m^2 of specifications)*
- No Detritiation system or scrubber presence for EV
- 100% of dusts mobilisation at the beginning of the sequence *(same runs at 50% of resuspension have been also performed)*.

Further ECART parametrical analyses, always presented in the following of this Chapter 4 and identified in Table 3.4, have been carried out about:

- Maximum EV leakages: 1% and 75% daily;
- Presence of a pool scrubber between VV and EV, with a constant DF equal to 0.9;
- Presence of a DS for the EV atmosphere, with a constant flow capacity of 3.0 kg/s and an efficiency of 99.9%.

4.1 Main Thermal-hydraulics Results

The pressurization time trends inside the whole PPCS system (VV and EV) are shown in Figure 4.1 for the reference case 0, where the three characteristic phases of the system pressurisation are quite evident:

a) **Helium pressurisation of the VV only**, before the rupture disk openings at 0.1 MPa, obviously dependent by the values of the VV free volume and of the helium flow rate.

b) **Discharge into the EV, trough the RD, until pressures equilibrium between VV and VV**, equilibrium pressure normally is coincident with the maximum values of the VV and EV total pressures. This value of the "equilibrium pressure" practically only depends by the system total free volume, with low influences by the leakages rates and by the helium flow-rate [Paci, 2003].

c) **Long term phase**, where the whole system has the same total pressure but different temperatures, with this pressure descending towards the atmospheric value, for the combined effect of the daily leakages and of the heat transfer with the EV structure.

The influence on the overall thermal-hydraulics transient of the scrubber presence is shown in Figure 4.2, with the comparison of the VV and EV total pressure results for cases 0 and 3. The presence of an 1.0 m depth scrubber pool does not allowed the airborne flow from VV to EV (and also the backflow) if the pressure difference between the two control nodes is lower than 0.1 bar. So, at the initial peak, there is a pressure difference of about 0.1 bar and also the long term phase of the sequence is quite different, with the two volumes depressurising with separate time histories.

The DS presence (case 6) and the EV leakages (case 1) obviously influence only the long term phase of the sequence (Figure 4.3), respectively decreasing the long term pressure for the DS cooling action and, on the contrary, increasing it with the reduction of the EV leakages.

Concluding, only for the case 3 (scrubber presence) the PPCS pressure trends are quite different from the reference analysis and the pressure peak no more coincident with the equilibrium value (Figure 4.4). However, it has to be highlighted as, also with this scrubber presence, the **capability of the PPCS Model B confinement design to withstand this "LOFA + in vessel LOCA" thermal-hydraulic transient it is trusted and it respects its final goal: the overpressure in the VV is safely mitigated under the design pressure of 0.2 MPa.**

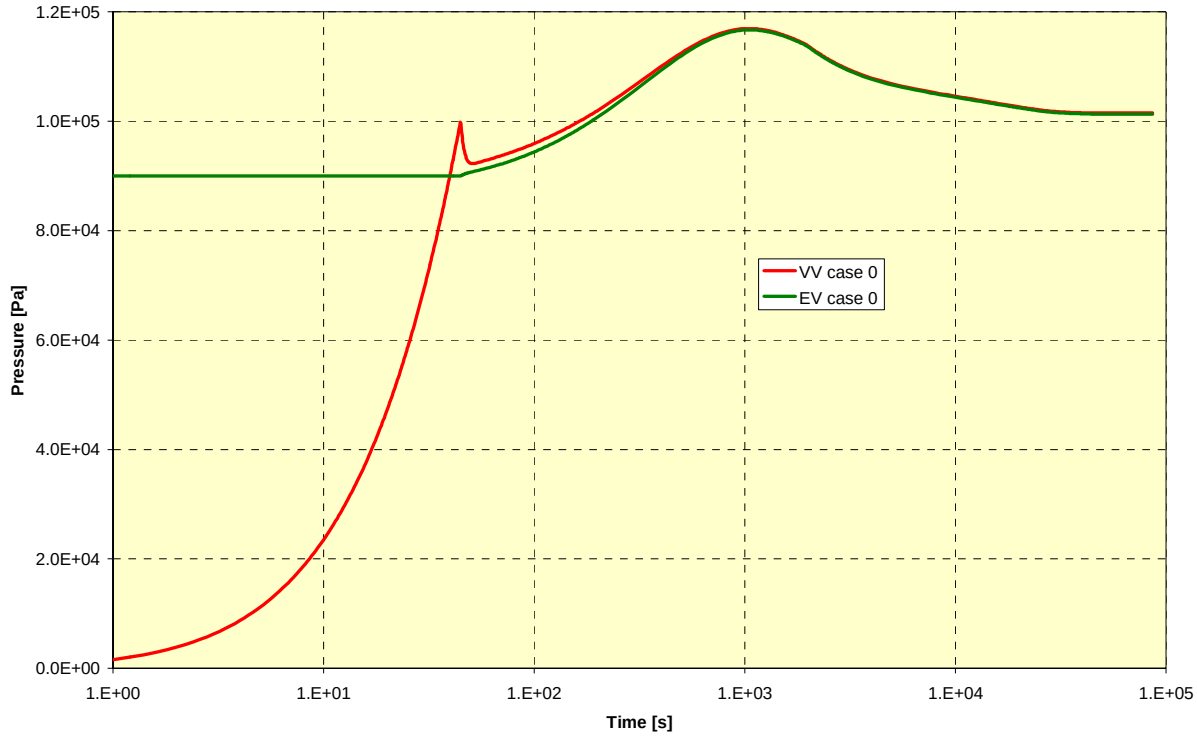

Figure 4.1: Pressure trends inside VV and EV (case 0).

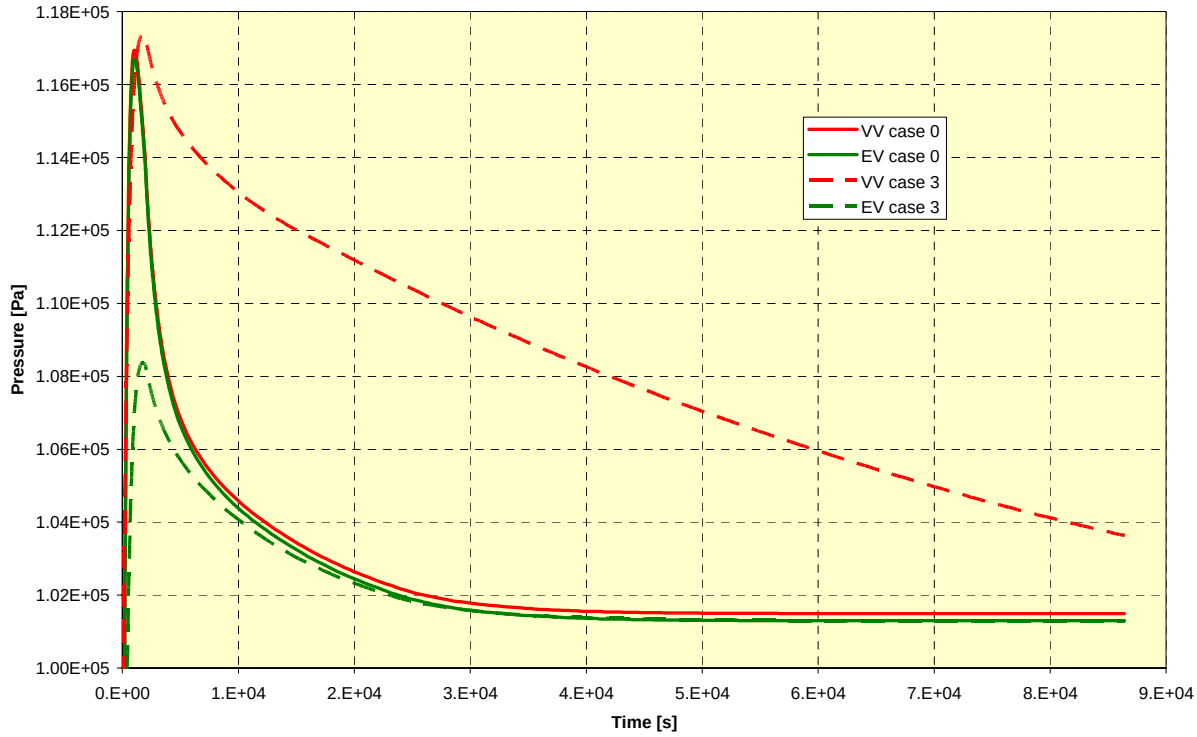

Figure 4.2: Cases 0 and 3- pressure trends inside VV and EV.

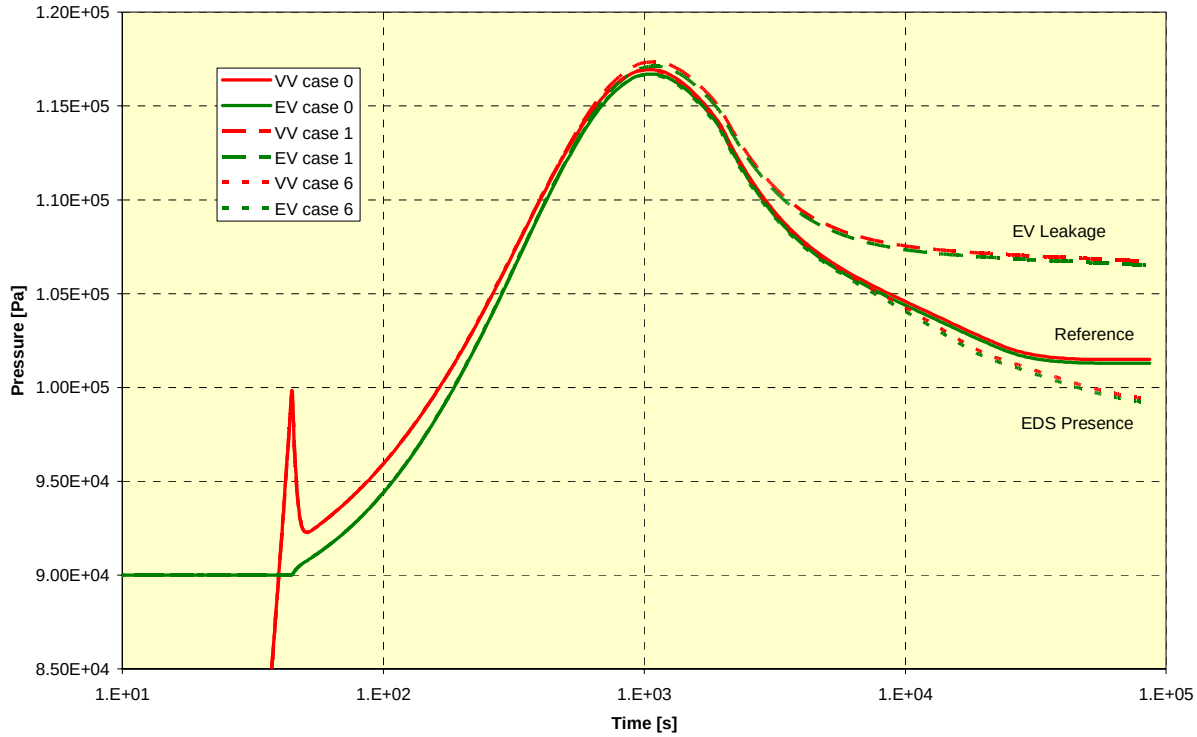

Figure 4.3: Cases 0, 1 and 6 - pressure trends inside VV and EV.

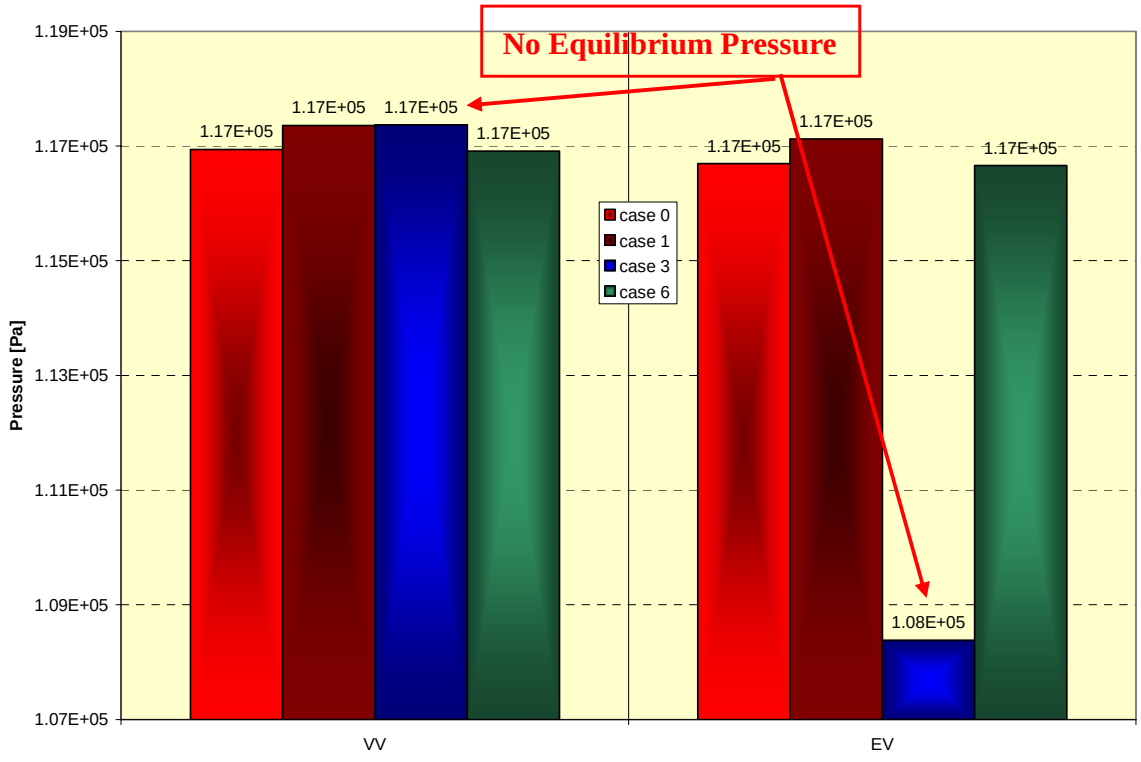

Figure 4.4: Parametrical analysis – VV and EV pressure maximum values.

As regards the internal surface temperatures (facing the VV) of the two PFC heat structures, no particular comment is needed: the initial transients of these temperatures are reported in Figure 3.3 while the long term trends are reported in Figure 4.5. While the FW is slowing approaching its thermal equilibrium, the cooled DV is always in thermal equilibrium with the imposed cooling fluid temperature.

Also for the VV and EV atmosphere temperature trends predicted by ECART (Figure 4.6) three different phenomenological phases are present:

1) the initial compression effect inside the VV atmosphere due to the helium blow-down, until the RD opening, is quite evident;
2) the subsequent VV cooling due to expansion phase of the compressed helium into the EV atmosphere, leading to at the EV temperature increase;
3) These initial two phases are followed by a long term thermal re-equilibrium with a decrease towards the final temperature levels, deriving from a balance of the atmosphere internal energy, thermal capacities/losses, mass exchanges between EV and VV and the DV cooling action.

The presence of the DS and the variation of EV leakage maximum rate have almost no practical influence on these VV and EV atmosphere temperature trends. On the contrary, only small effects are evident due to the scrubber pool presence (Figure 4.6), again for the inhibition of the long term mass exchanges at the RD between VV and EV. With the scrubber, the temperature increase for the EV atmosphere at the RD opening is lower while the final equilibrium temperature of the VV atmosphere is the DV surface one (not lower as in the reference run 0 for the cold air mass back flowing from the cold EV atmosphere to the hot VV one).

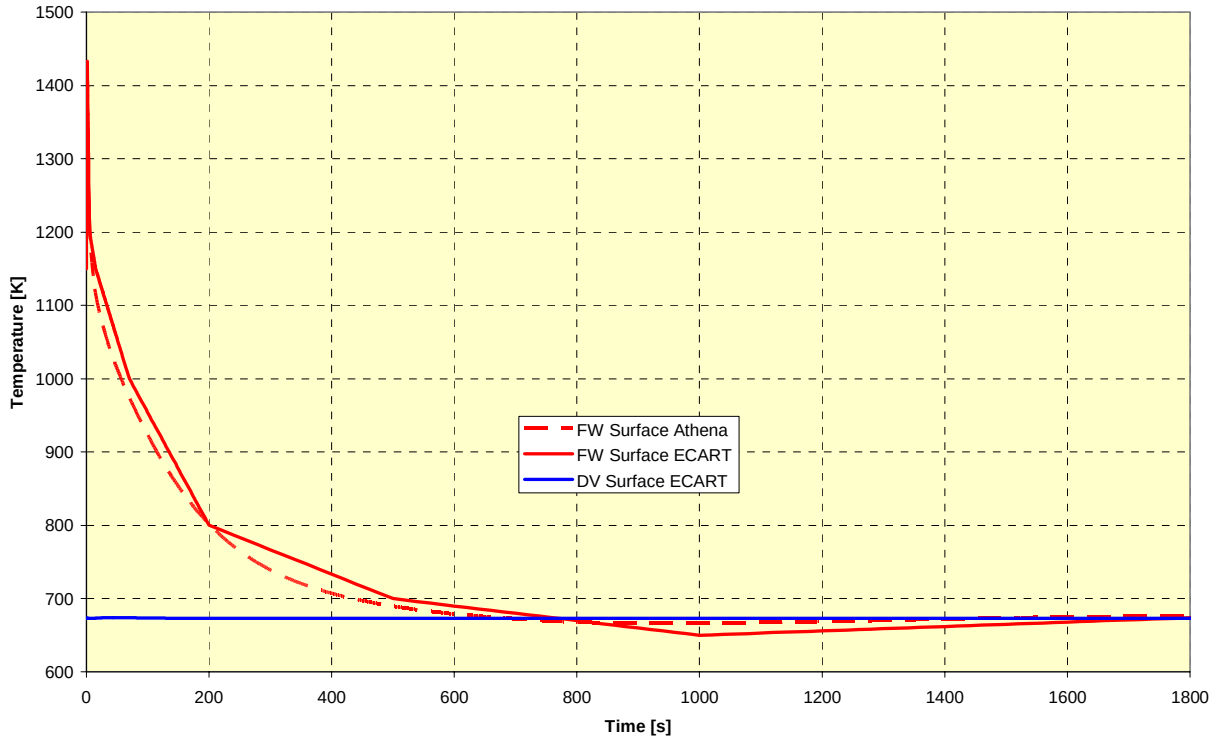

Figure 4.5: PFCs temperatures in the long term phase.

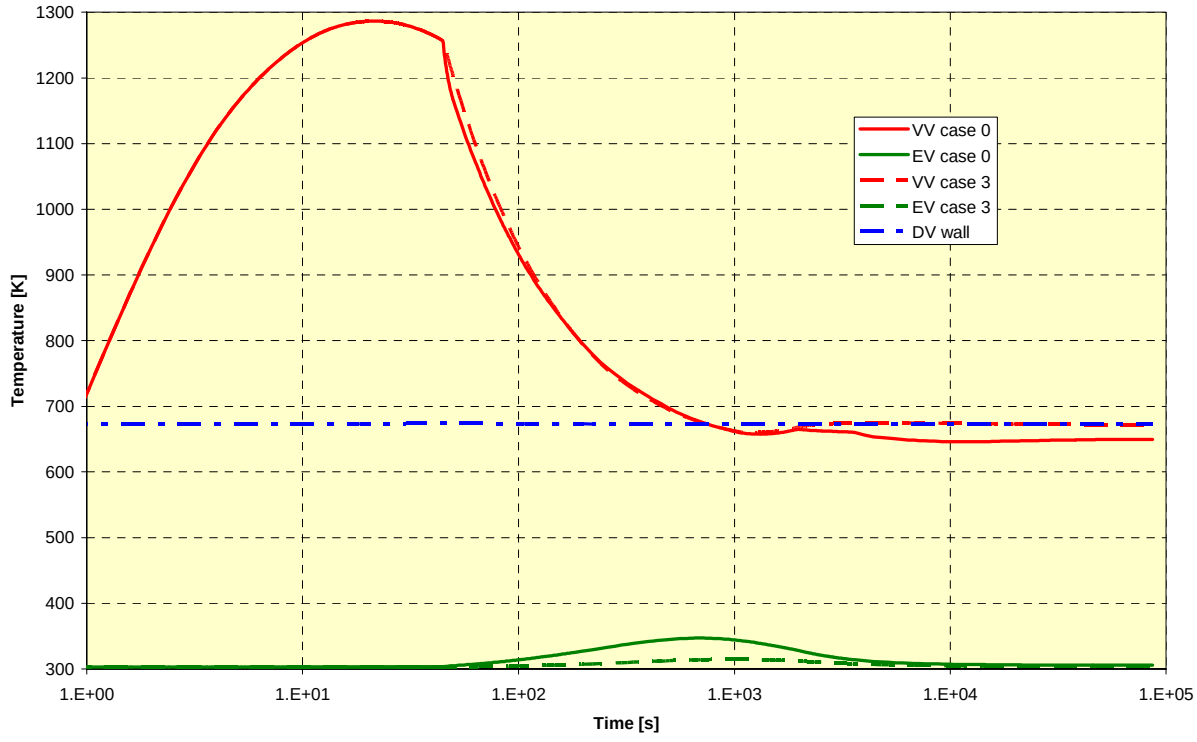

Figure 4.6: Atmosphere temperatures.

4.2 Environmental Release Results

Besides the thermal-hydraulics transient, as previously highlighted, ECART is also able to assess the environmental releases of both W and SS dusts and tritium gas, considering also possible retention phenomena. The results of the ECART aerosol models, already tested and validated in the framework of fission reactor studies [Wright, 1994], [Jones, 2001], are also promising in the fusion safety field [Cambi, 2002].

Summarizing the previous achieved PCCS results [Paci, 2003] about the releases to the outside environment for analysed Model B sequence, ECART predicts **large amounts of the initial inventories as dispersed after 24 h from the beginning of the accident**, mainly due to the high daily leakage (75%) of the EV. These results were considered as indicative of the **incapacity of the PPCS confinement Model B to cope with this relevant accident scenario maintaining the original specifications**. However, these extremely high fractions of the tritium and dusts inventories released to the external environment that represent in [Paci, 2003] the solution of the source term problem (and reported for the reference case 0 in Figure 4.7), could be considerably reduced employing a DS and/or increasing the tightness of the EV as shown in the same report.

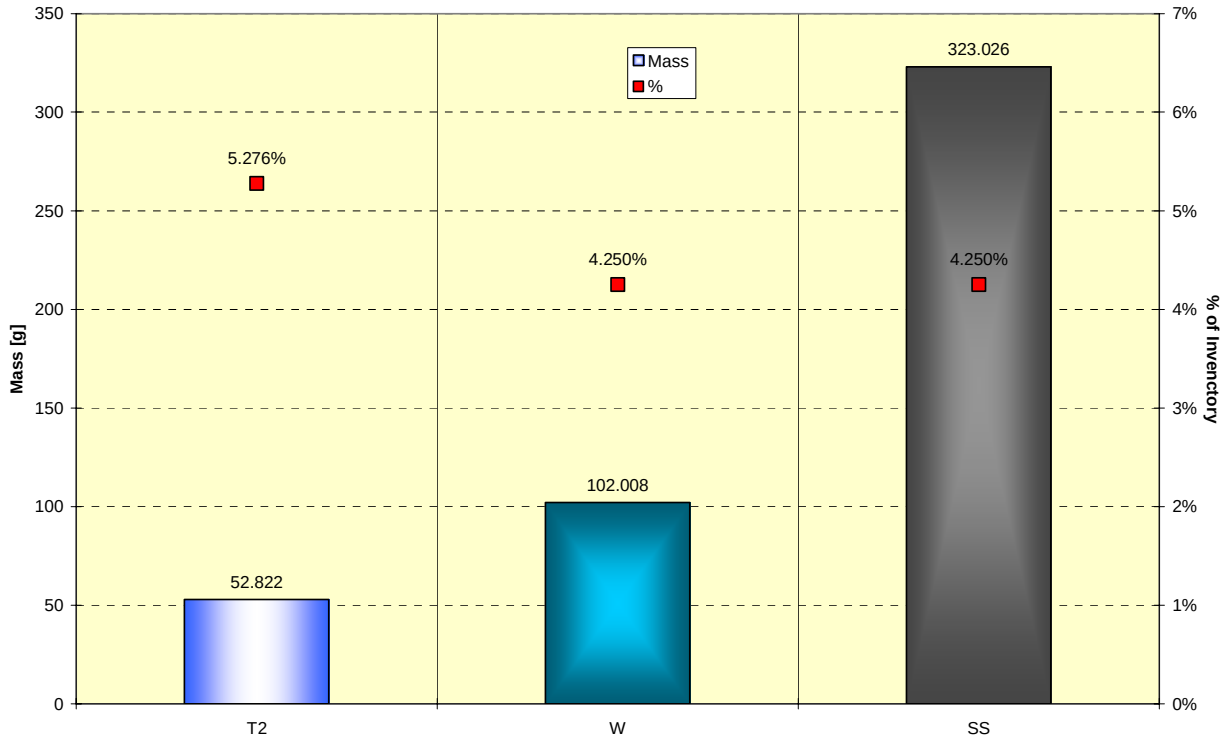

Figure 4.7: Releases of radioactive species to the environment for the reference case 0.

Starting from these considerations, during the Meeting [ENEA, 2003] was decided to carry out further in deep analysis of the PPCS external releases, considering the possible presence of mitigation actions, previously discussed in Paragraph 3.2, (i.e., DS for EV, pool scrubber at RD, increase of the EV tightness) plus analysing the influence of the fraction of dust particles initially resuspended inside the VV (100% or 50%). The 16 parametrical analyses performed, deriving from the different combinations of the mitigation actions, are reported in the previous Table 3.4 repeated in Table 4.1 while, in the following of the present report, the results for the external releases of these 16 parametrical runs will be analyzed.

	EDS	lkg	Scrub	risosp		EDS	lkg	Scrub	risosp
reference	no	75%	no	100%	6	3.0	75%	no	100%
1		1			7		1		
2		75		50	8		75		50
3			yes	100	9			yes	100
3r				50	9r				50
4		1		100	10		1		100
4r				50	10r				50
5			no	50	11			no	50

Table 4.1: Performed parametrical analysis.

Starting from the tritium gas results, it is necessary to highlight as the tritium transport is considered by ECART to occur with no depletion mechanisms. Its retention within the PPCS plant is then mainly due to the tightness of the system and in particular of the EV. Parametrical analysis (runs 0 and 1, 6 and 7, respectively without and with the DS presence) have been carried out on this aspect and the comparison of the results about the tritium releases is reported in Figure 4.8. Obviously, increasing the EV tightness from 75% to 1% (case 0 to case 1, case 6 to case 7), the released tritium fraction fm EV (EXTEV) decreased until about 0.3% of the total amount for a daily leakage equal to 1% of the EV free volume, without DS, and to about 0.08% with DS. This is equivalent to about 3. g or 0.8 g of tritium, as reported in Figure 4.9, where all the tritium masses released into the EXTEV for the 16 different parametrical analysis are reported. For EXTVV (tritium release directly from VV) these masses are reported in Figure 4.10, where an increase of the tritium released masses from VV is highlighted with the decrease of the EV leakages, due to the correspondent small increase of the VV pressure level (Figure 4.11).

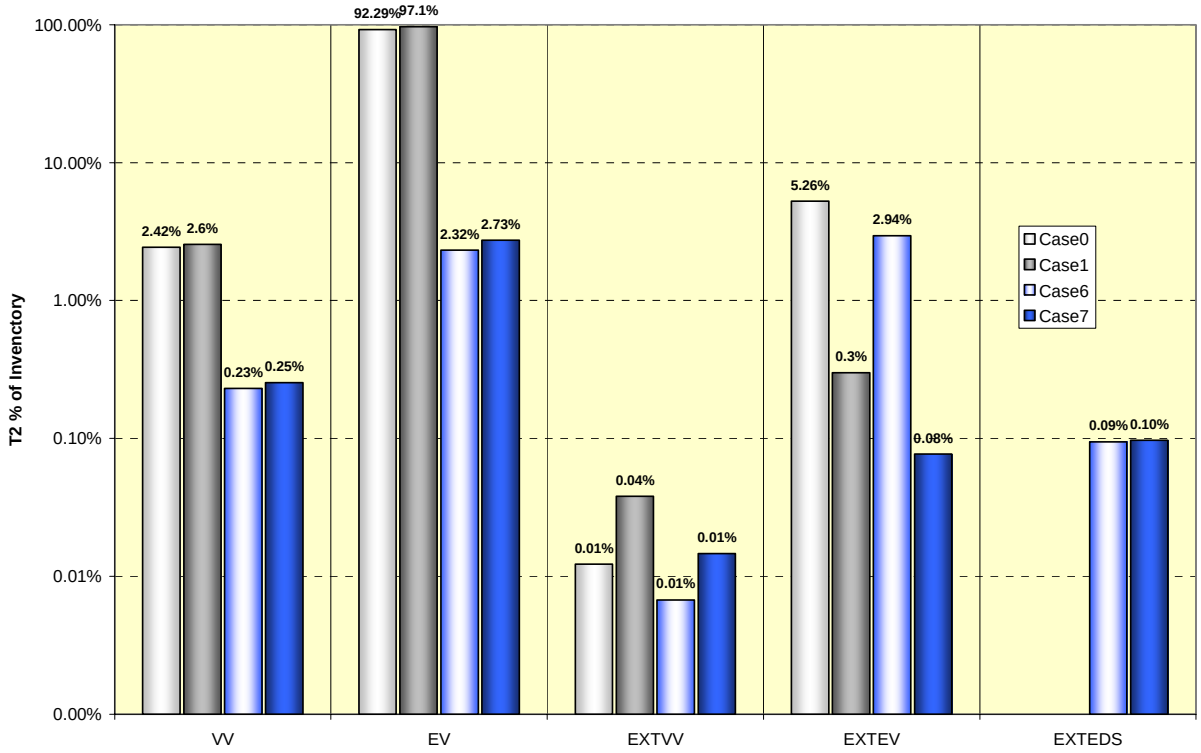

Figure 4.8: Parametrical analysis on EV leakages: Tritium releases.

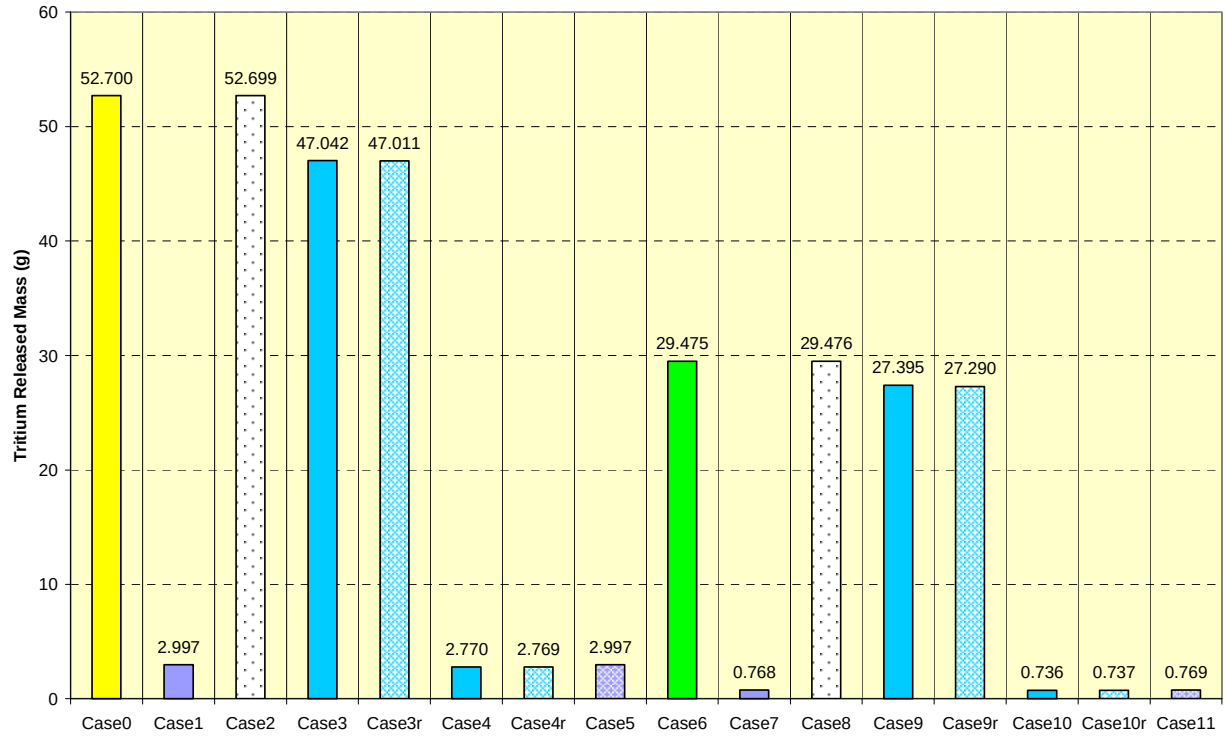

Figure 4.9: Parametrical analysis: tritium releases into EXTEV.

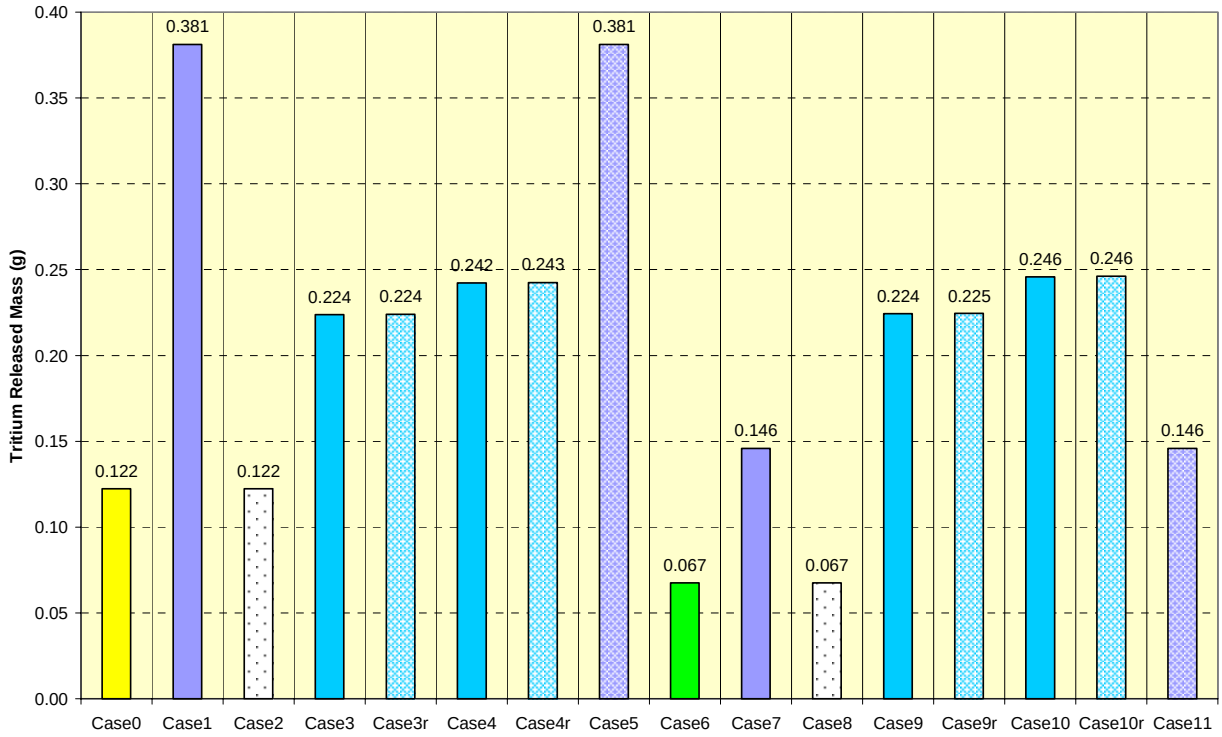

Figure 4.10: Parametrical analysis: Tritium releases into EXTVV.

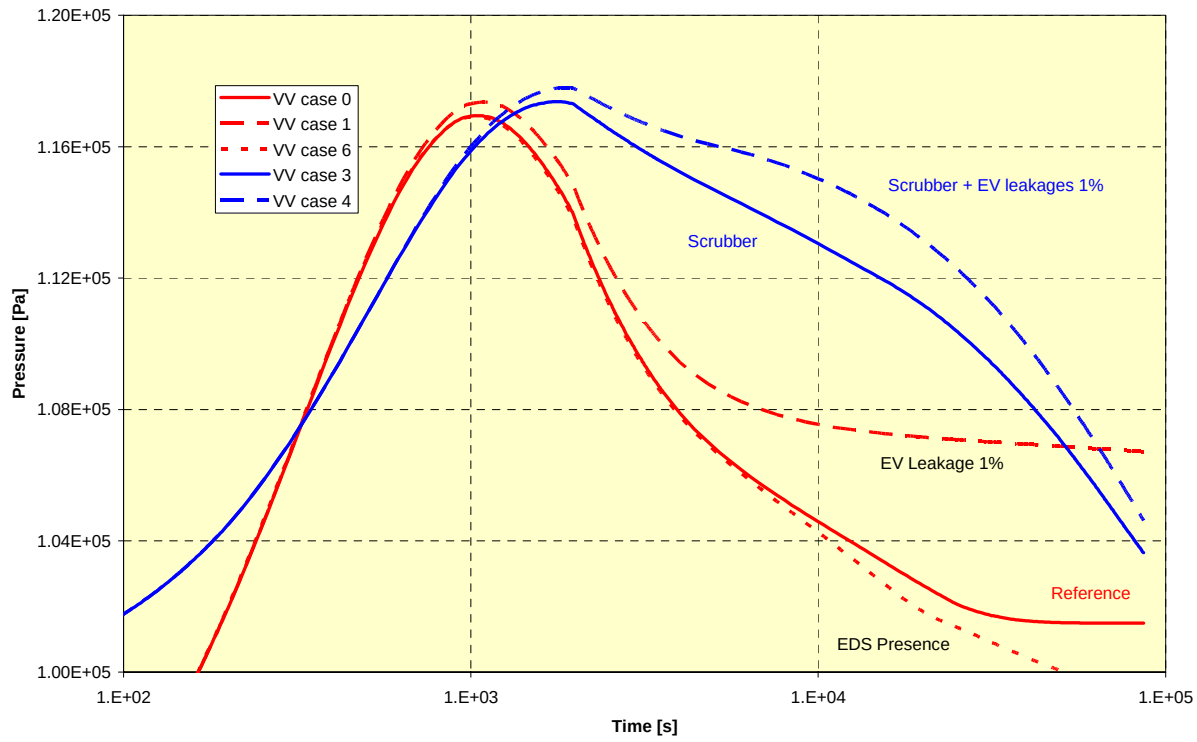

Figure 4.11: Parametrical analysis on VV maximum pressure.

Cleary the scrubber presence (case 3 and case 4, with EV daily leakages 1%), increasing the pressure level inside the VV (Figure 4.11) and decreasing the EV one (Figure 4.12), also changes the tritium gas releases, increasing the VV ones but reducing the higher EV ones. On the contrary, no influence is obviously predicted for the changing of the dust resuspended fraction.

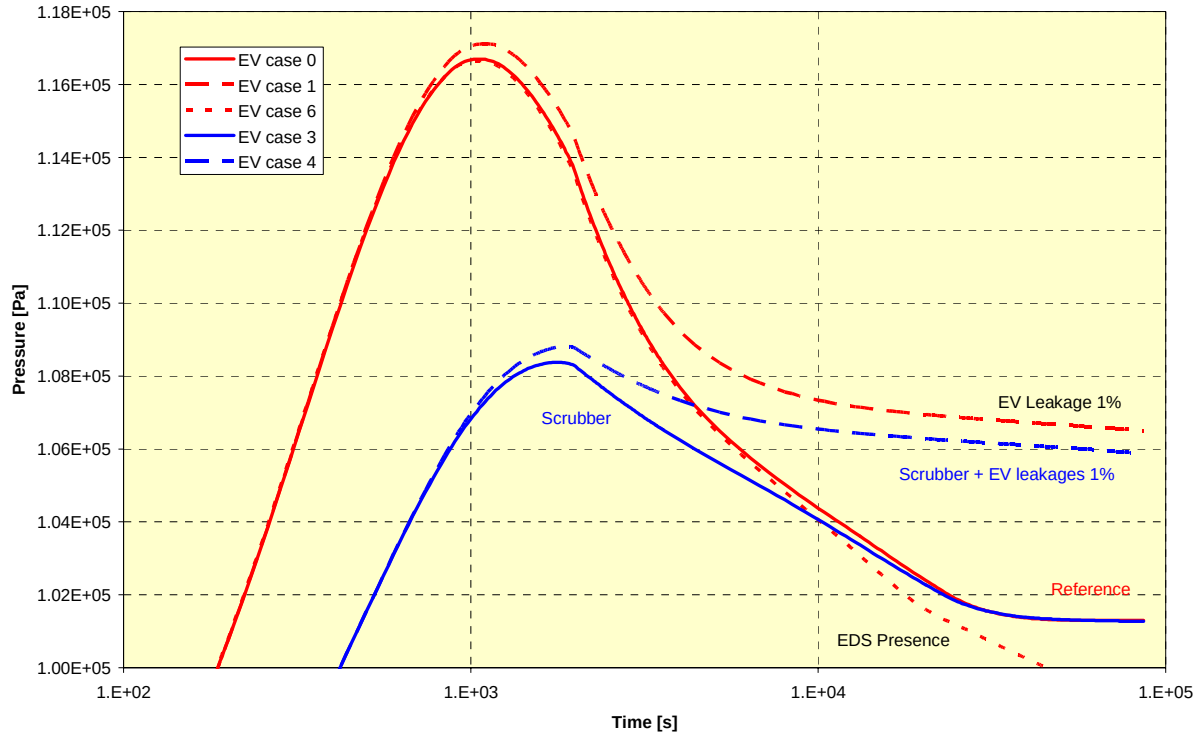

Figure 4.12: Parametrical analysis on EV maximum pressure.

A further problem, highlighted in Figure 4.8, is the high quantity of the tritium mass trapped inside the EV atmosphere at 24 hours. Also with the higher EV daily leakage (75%), over the 92% of Tritium inventory remains inside this large volume at the end of the sequence. To reduce this quantity, and especially to reduce the external dangerous releases, the use of a Detritiation System (DS) has been foreseen. Obviously, the DS presence has an influence, small but not negligible for a 24 hours transient, also on the long term thermal-hydraulic behaviour of the system, in particular on the equilibrium total pressure, as reported in Figure 4.13 for the EV pressure trend.

Concluding the tritium releases analysis, the total external releases results, expressed in grams, for the 16 parametrical runs are summarised in Figure 4.14.

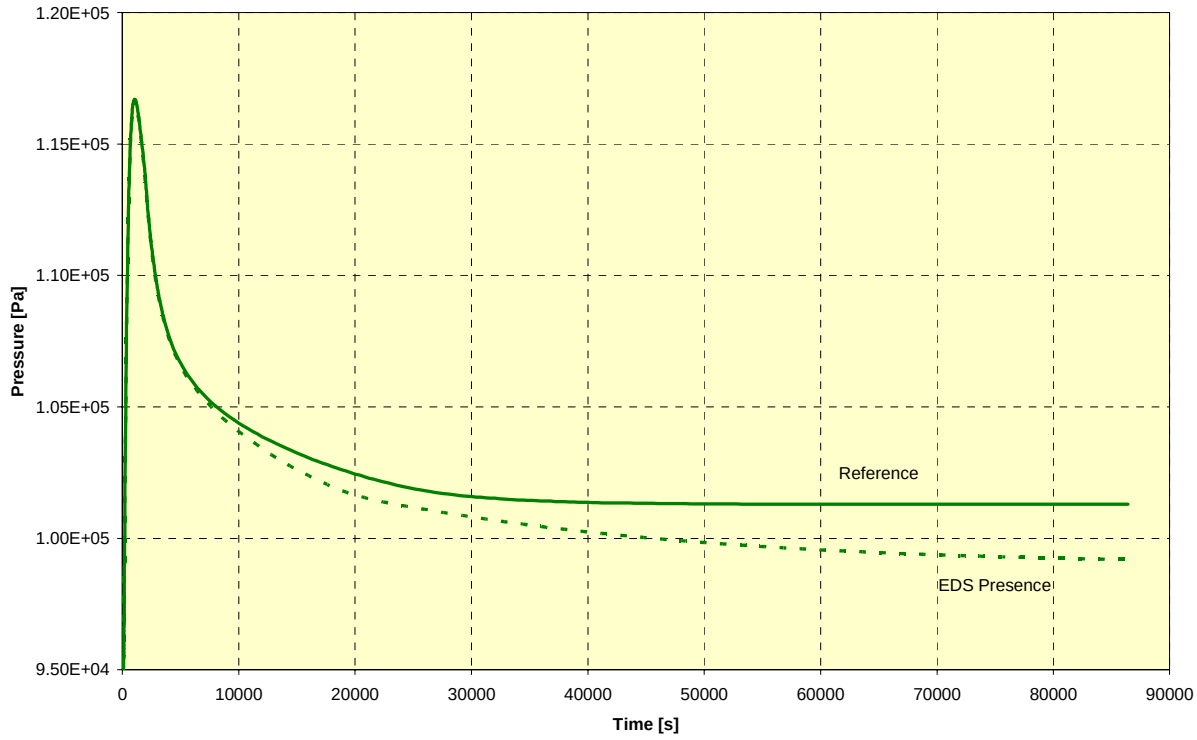

Figure 4.13: Parametrical analysis on DS (3.0 kg/s): EV Pressures.

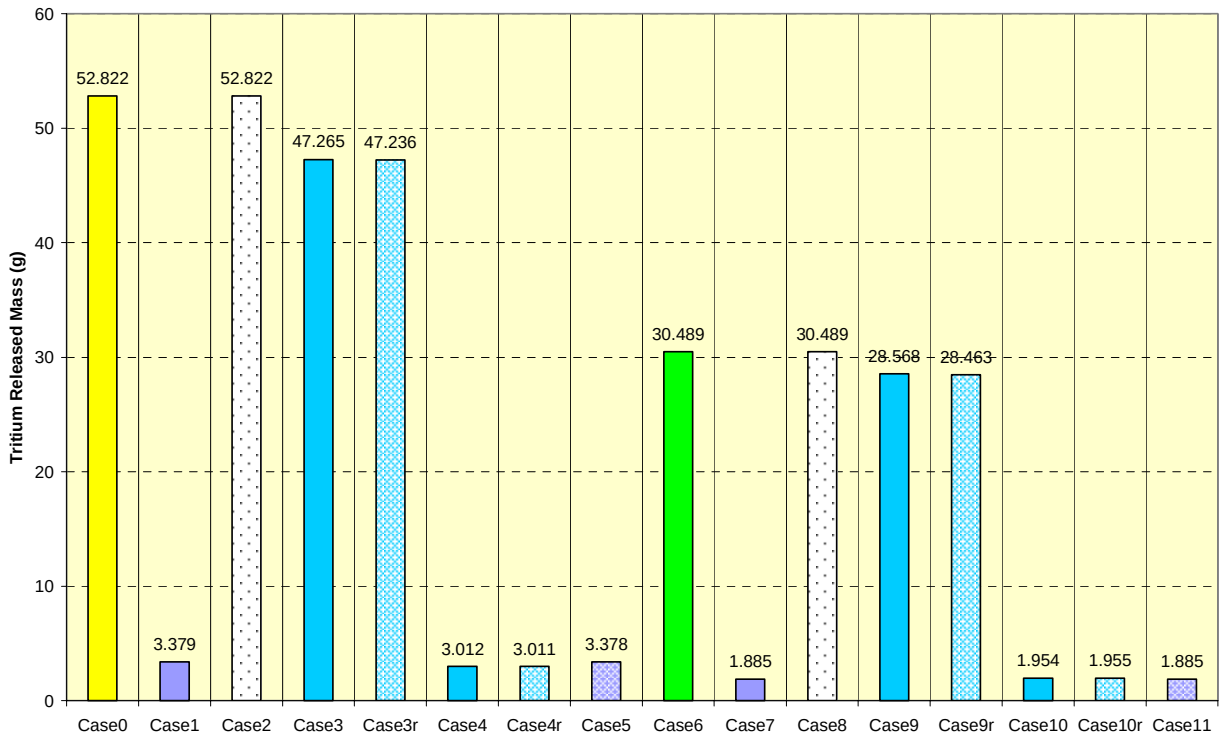

Figure 4.14: Results of the parametrical analysis on total tritium releases.

The same considerations made for the tritium gas releases can be done also for the W and SS dusts releases (Figure 4.15 and Figure 4.16, respectively without and with the DS presence), with too high values of the PPCS dust releases predicted by ECART, as the tritium one, in the reference analysis "case 0". The dust particles behaviour is the same for the two species, being the same the initial granulometry, input imposed, so only one fraction of the initial inventory is reported, applicable for both W and SS dusts.

It has to be immediately highlighted as, for the PPCS dusts, the stronger reduction factor is linked to the scrubber presence: a reduction of about two orders of magnitude is calculated for the dust releases from the EV, also for the low EV tightness (case 3), shifting the level of the EV dust releases to the lower VV ones. **So the desirable strong reduction of the dust external releases could be obtained simply introducing the scrubber presence, after the RD between VV and EV, in the PPCS design**.

It has to be remembered that the dusts particles are assumed suspended into the VV atmosphere at the beginning of the transient and, consequently, the global behaviour of this particles release is quite similar to the gaseous tritium one, with only the retention in the EV and VV, mainly for gravitational deposition, and for the possible scrubber presence. Investigations are under way [Parozzi, 2002], [Porfiri, 2003a] to estimate a realistic initial mobilisation (i.e. the re-suspension fraction) of the VV dust inventory, in reality initially deposited on the VV walls and not suspended in its atmosphere. For the present analysis, these dusts have been considered as homogeneously suspended (100% as total fraction of resuspension) inside the VV atmosphere at the beginning of the helium release, as conservative assumption. However, all the analysis have been also performed considering only the 50% of the dust resuspended (runs 2, 3r, 4r, 5, 8, 9r, 10r, 11). The results of this 50% reduction are highlighted in Figure 4.17 for SS (but qualitatively are the same also for W), where on half of the external dust releases is predicted for the cases with the 50% of VV resuspension. **Practically, the total external releases of dusts are reduced of the same quantity of the reduction for the resuspended fraction inside the VV**.

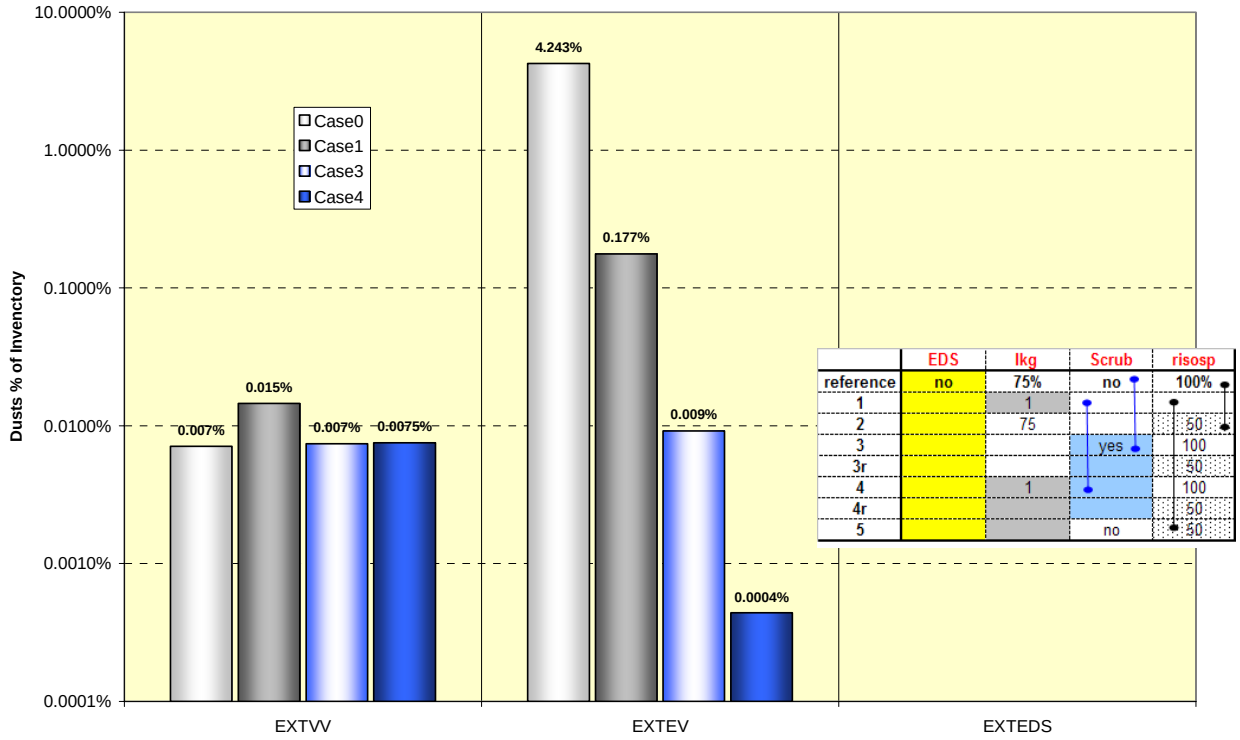

Figure 4.15: Parametrical analysis on EV leakages and scrubber: dusts releases (no DS).

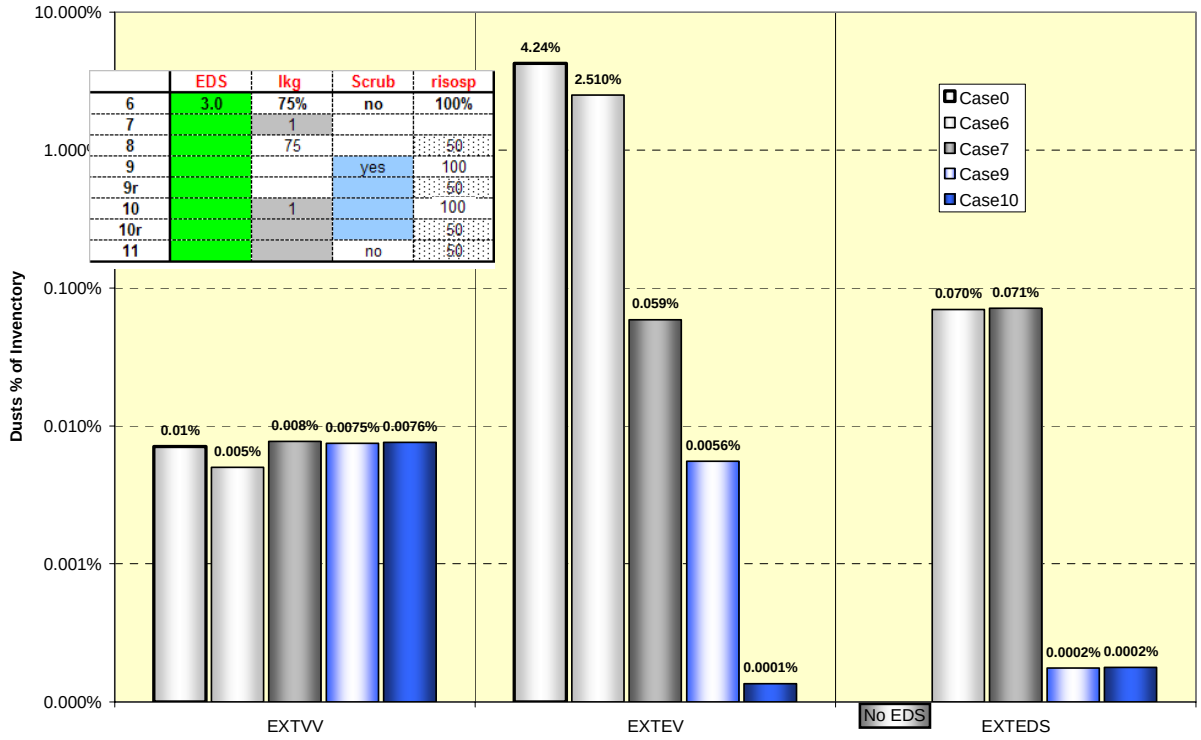

Figure 4.16: Parametrical analysis on EV leakages and scrubber presence: dusts releases (DS).

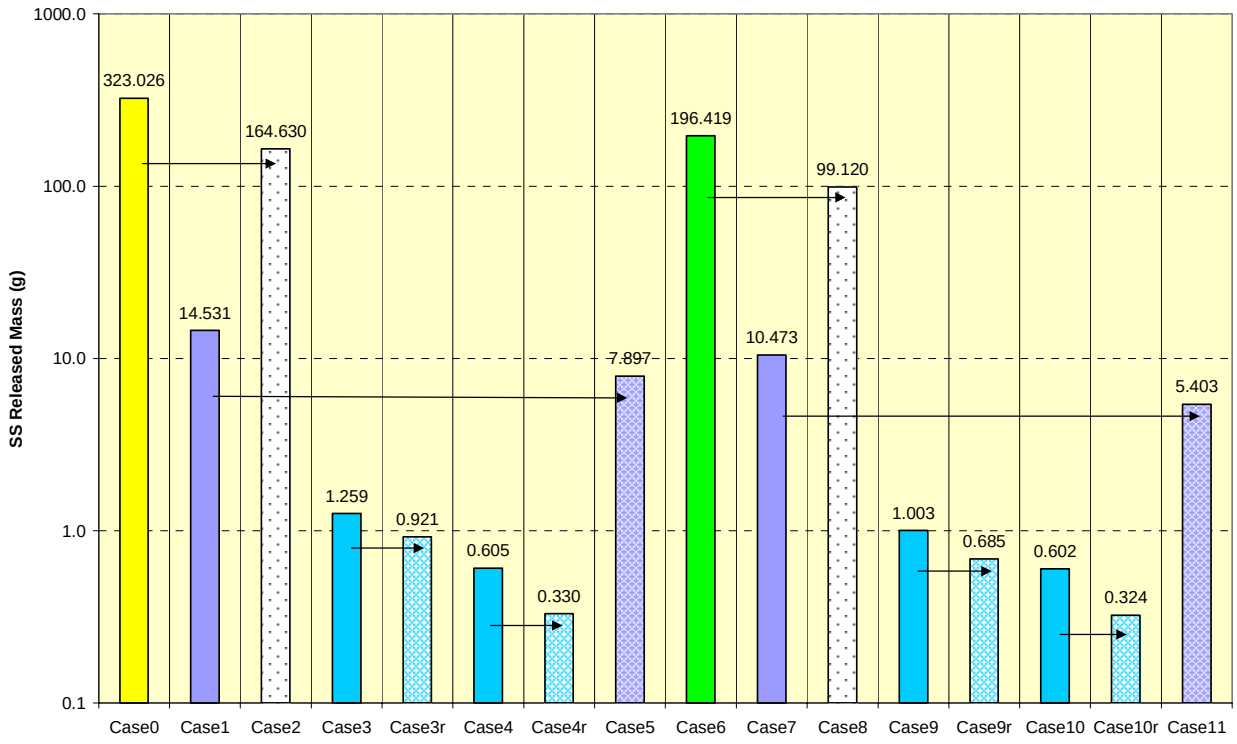

Figure 4.17: Parametrical analysis on influence of resuspended fraction on dusts releases.

Concluding this analysis on tritium gas and dusts behaviours for PCCS Model B, a summary of the total mass releases, expressed in grams, for the 16 parametrical runs is reported in the Table 4.2 and Table 4.3, respectively not considering and considering the presence of a DS for the EV with efficiency 99.9% and a flow-rate of 3.0 kg/s. The following Table 4.4 and Table 4.5 are equivalent to the previous two ones but the radioactive releases are expressed in percentage of the initial mass inventory. In these 4 tables, the mass quantities and percentages are referred to tritium and dusts masses suspended in the atmosphere of the control volumes.

run	Case0	Case1	Case2	Case3	Case3r	Case4	Case4r	Case5
VV	24.250	25.537	24.249	1.666	1.666	1.686	1.686	25.537
EV	923.928	972.085	923.929	952.069	952.098	996.302	996.303	972.085
EXTVV	0.122	0.381	0.122	0.224	0.224	0.242	0.243	0.381
EXTEV	52.700	2.997	52.699	47.042	47.011	2.770	2.769	2.997
T2	**52.822**	**3.379**	**52.822**	**47.265**	**47.236**	**3.012**	**3.011**	**3.378**
VV	9.041	9.533	6.167	0.010	0.008	0.009	0.007	6.521
EV	745.891	781.036	459.031	2.684	2.612	2.795	2.726	481.734
EXTVV	0.170	0.349	0.090	0.177	0.093	0.181	0.094	0.198
EXTEV	101.838	4.240	51.898	0.220	0.198	0.011	0.010	2.296
W	**102.008**	**4.589**	**51.988**	**0.397**	**0.291**	**0.191**	**0.104**	**2.494**
VV	28.629	30.187	19.529	0.033	0.026	0.029	0.023	20.650
EV	2361.988	2473.280	1453.599	8.499	8.270	8.849	8.633	1525.492
EXTVV	0.540	1.105	0.286	0.562	0.293	0.572	0.299	0.627
EXTEV	322.486	13.426	164.343	0.697	0.628	0.033	0.031	7.270
SS	**323.026**	**14.531**	**164.630**	**1.259**	**0.921**	**0.605**	**0.330**	**7.897**

Table 4.2: Total tritium and dusts external releases in grams (no DS).

(In red character environmental releases)

run	Case6	Case7	Case8	Case9	Case9r	Case10	Case10r	Case11
VV	2.304	2.539	2.304	1.679	1.679	1.701	1.702	2.539
EV	23.257	27.350	23.256	22.796	22.796	26.900	26.909	27.350
EXTVV	0.067	0.146	0.067	0.224	0.225	0.246	0.246	0.146
EXTEV	29.475	0.768	29.476	27.395	27.290	0.736	0.737	0.769
EXTEDS	0.946	0.970	0.946	0.949	0.949	0.971	0.971	0.970
T2	**30.489**	**1.885**	**30.489**	**28.568**	**28.463**	**1.954**	**1.955**	**1.885**
VV	0.600	0.688	0.405	0.011	0.008	0.009	0.007	0.463
EV	20.059	23.723	11.700	0.063	0.061	0.073	0.071	13.853
EXTVV	0.120	0.185	0.062	0.179	0.093	0.183	0.095	0.099
EXTEV	60.229	1.410	30.374	0.133	0.119	0.003	0.003	0.724
EXTEDS	1.678	1.711	0.866	0.004	0.004	0.004	0.004	0.884
W	**62.027**	**3.307**	**31.301**	**0.317**	**0.216**	**0.190**	**0.102**	**1.706**
VV	1.901	2.177	1.283	0.033	0.027	0.029	0.023	1.468
EV	63.519	75.123	37.051	0.198	0.192	0.232	0.226	43.867
EXTVV	0.380	0.587	0.195	0.567	0.296	0.578	0.302	0.313
EXTEV	190.726	4.466	96.184	0.422	0.377	0.010	0.009	2.291
EXTEDS	5.313	5.420	2.741	0.013	0.012	0.013	0.012	2.798
SS	**196.419**	**10.473**	**99.120**	**1.003**	**0.685**	**0.602**	**0.324**	**5.403**

Table 4.3: Total tritium and dusts external releases in grams (DS).

(In red character environmental releases)

run	Case0	Case1	Case2	Case3	Case3r	Case4	Case4r	Case5
VV	2.422%	2.551%	2.422%	0.166%	0.166%	0.168%	0.168%	2.551%
EV	92.291%	97.102%	92.291%	95.102%	95.105%	99.521%	99.521%	97.102%
EXTVV	0.012%	0.038%	0.012%	0.022%	0.022%	0.024%	0.024%	0.038%
EXTEV	5.264%	0.299%	5.264%	4.699%	4.696%	0.277%	0.277%	0.299%
T2	**5.276%**	**0.337%**	**5.276%**	**4.721%**	**4.718%**	**0.301%**	**0.301%**	**0.337%**
VV	0.377%	0.397%	0.257%	0.000%	0.000%	0.000%	0.000%	0.272%
EV	31.079%	32.543%	19.126%	0.112%	0.109%	0.116%	0.114%	20.072%
EXTVV	0.007%	0.015%	0.004%	0.007%	0.004%	0.008%	0.004%	0.008%
EXTEV	4.243%	0.177%	2.162%	0.009%	0.008%	0.000%	0.000%	0.096%
W	**4.250%**	**0.191%**	**2.166%**	**0.017%**	**0.012%**	**0.008%**	**0.004%**	**0.104%**
VV	0.377%	0.397%	0.257%	0.000%	0.000%	0.000%	0.000%	0.272%
EV	31.079%	32.543%	19.126%	0.112%	0.109%	0.116%	0.114%	20.072%
EXTVV	0.007%	0.015%	0.004%	0.007%	0.004%	0.008%	0.004%	0.008%
EXTEV	4.243%	0.177%	2.162%	0.009%	0.008%	0.000%	0.000%	0.096%
SS	**4.250%**	**0.191%**	**2.166%**	**0.017%**	**0.012%**	**0.008%**	**0.004%**	**0.104%**

Table 4.4: Total percentage tritium and dusts external releases (no DS).

(In red character environmental releases)

run	Case6	Case7	Case8	Case9	Case9r	Case10	Case10r	Case11
VV	0.230%	0.254%	0.230%	0.168%	0.168%	0.170%	0.170%	0.254%
EV	2.323%	2.732%	2.323%	2.277%	2.277%	2.687%	2.688%	2.732%
EXTVV	0.007%	0.015%	0.007%	0.022%	0.022%	0.025%	0.025%	0.015%
EXTEV	2.944%	0.077%	2.944%	2.736%	2.726%	0.074%	0.074%	0.077%
EXTEDS	0.094%	0.097%	0.094%	0.095%	0.095%	0.097%	0.097%	0.097%
T2	**3.046%**	**0.188%**	**3.046%**	**2.854%**	**2.843%**	**0.195%**	**0.195%**	**0.188%**
VV	0.025%	0.029%	0.017%	0.000%	0.000%	0.000%	0.000%	0.019%
EV	0.836%	0.988%	0.488%	0.003%	0.003%	0.003%	0.003%	0.577%
EXTVV	0.005%	0.008%	0.003%	0.007%	0.004%	0.008%	0.004%	0.004%
EXTEV	2.510%	0.059%	1.266%	0.006%	0.005%	0.000%	0.000%	0.030%
EXTEDS	0.070%	0.071%	0.036%	0.000%	0.000%	0.000%	0.000%	0.037%
W	**2.584%**	**0.138%**	**1.304%**	**0.013%**	**0.009%**	**0.008%**	**0.004%**	**0.071%**
VV	0.025%	0.029%	0.017%	0.000%	0.000%	0.000%	0.000%	0.019%
EV	0.836%	0.988%	0.488%	0.003%	0.003%	0.003%	0.003%	0.577%
EXTVV	0.005%	0.008%	0.003%	0.007%	0.004%	0.008%	0.004%	0.004%
EXTEV	2.510%	0.059%	1.266%	0.006%	0.005%	0.000%	0.000%	0.030%
EXTEDS	0.070%	0.071%	0.036%	0.000%	0.000%	0.000%	0.000%	0.037%
SS	**2.584%**	**0.138%**	**1.304%**	**0.013%**	**0.009%**	**0.008%**	**0.004%**	**0.071%**

Table 4.5: Total percentage tritium and dusts external releases (DS).

(In red character environmental releases)

The same total releases results for the 16 parametrical runs are also summarised in Figure 4.14, Figure 4.18 and Figure 4.19, respectively for tritium gas, W dust and SS dust (releases expressed in grams) and in Figure 4.20 and Figure 4.21, respectively for Tritium and dusts releases expressed as percentage of the initial mass inventory (again for the WW dust and SS dust an unique plot is sufficient, being the same the two fractional releases, as above discussed).

Shortly summarising the performed work and the ECART results, the following two highlights related to the total external radioactive releases for the PPCS Model B, have to be mentioned in particular:

- the quite strong reduction of the external tritium releases obtained with the combined adoption of a DS for the EV atmosphere and the contemporary increase of the EV tightness to 1% daily of the EV total free volume at the design pressure (the calculated reduction is from about 5% to about 0.2% of the initial inventory of the gas mass);
- the very strong reduction of the dust releases simply with the adoption of a pool scrubber, after the RD between the VV and VV, also without reducing the EV tightness and without DS presence (the calculated reduction is from about 4% to about 0.02% of the initial inventory of the two dusts).

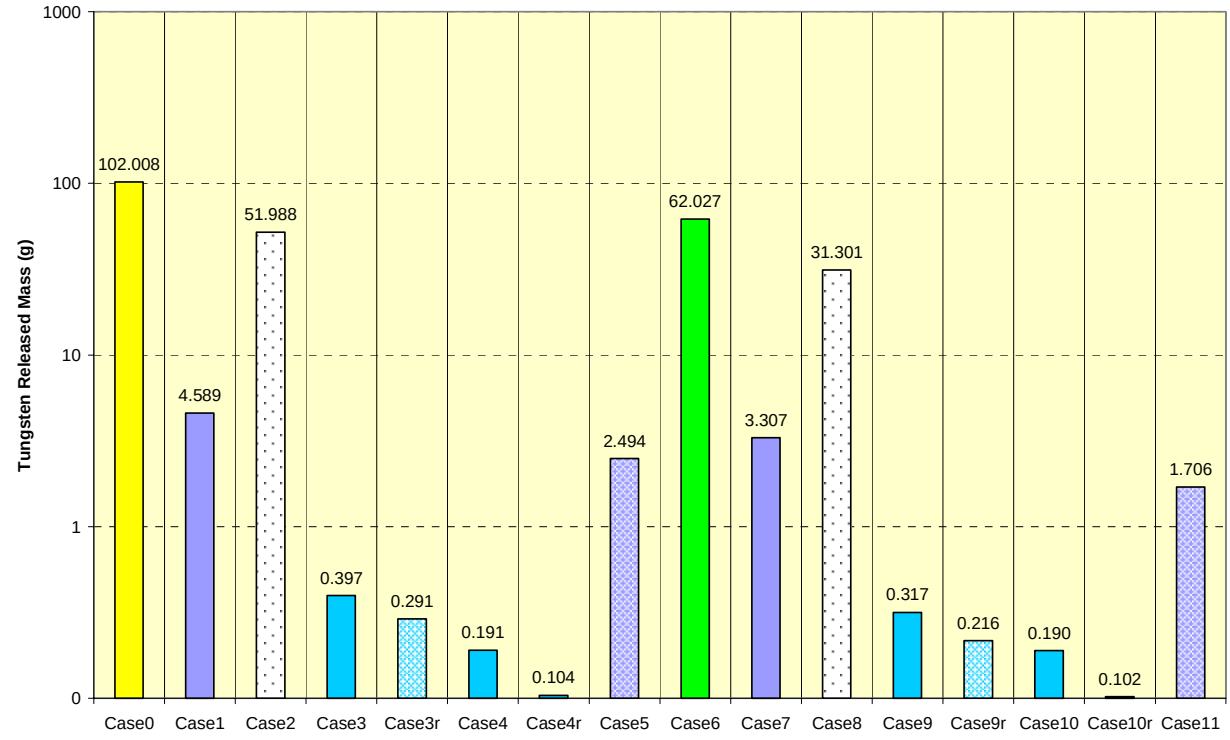

Figure 4.18: Parametrical analysis: Total W releases.

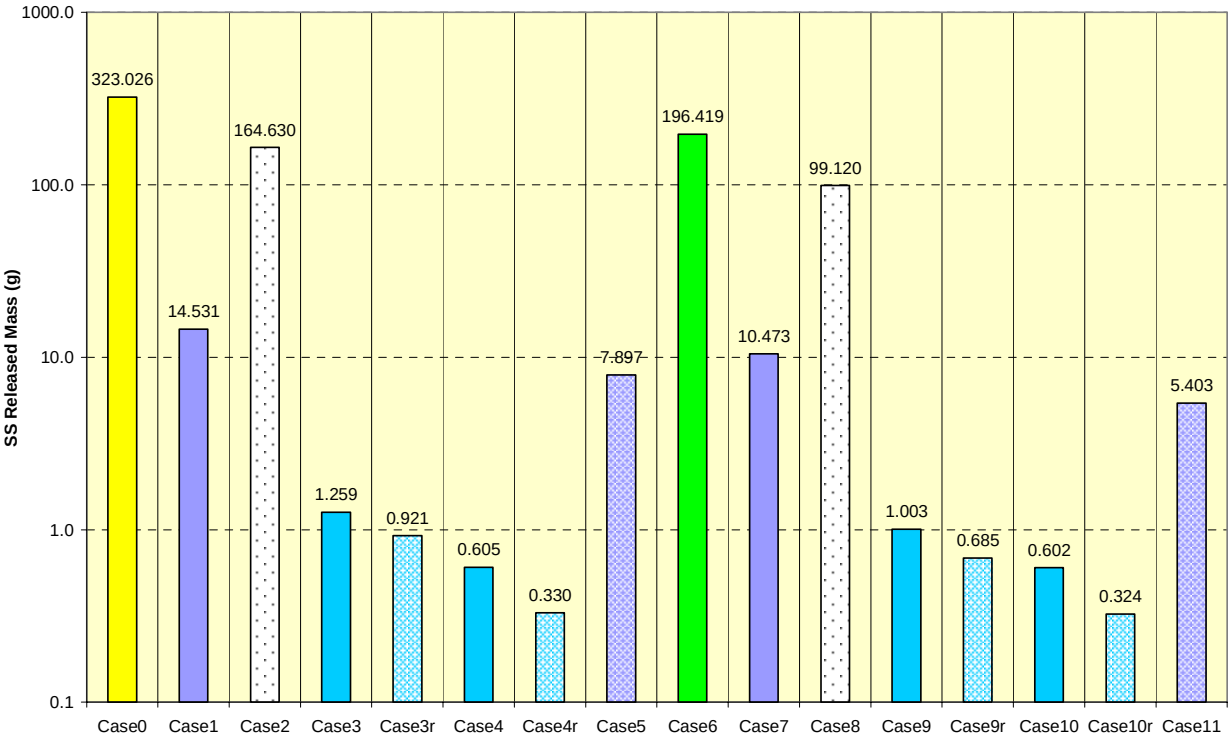

Figure 4.19: Parametrical analysis: Total SS releases.

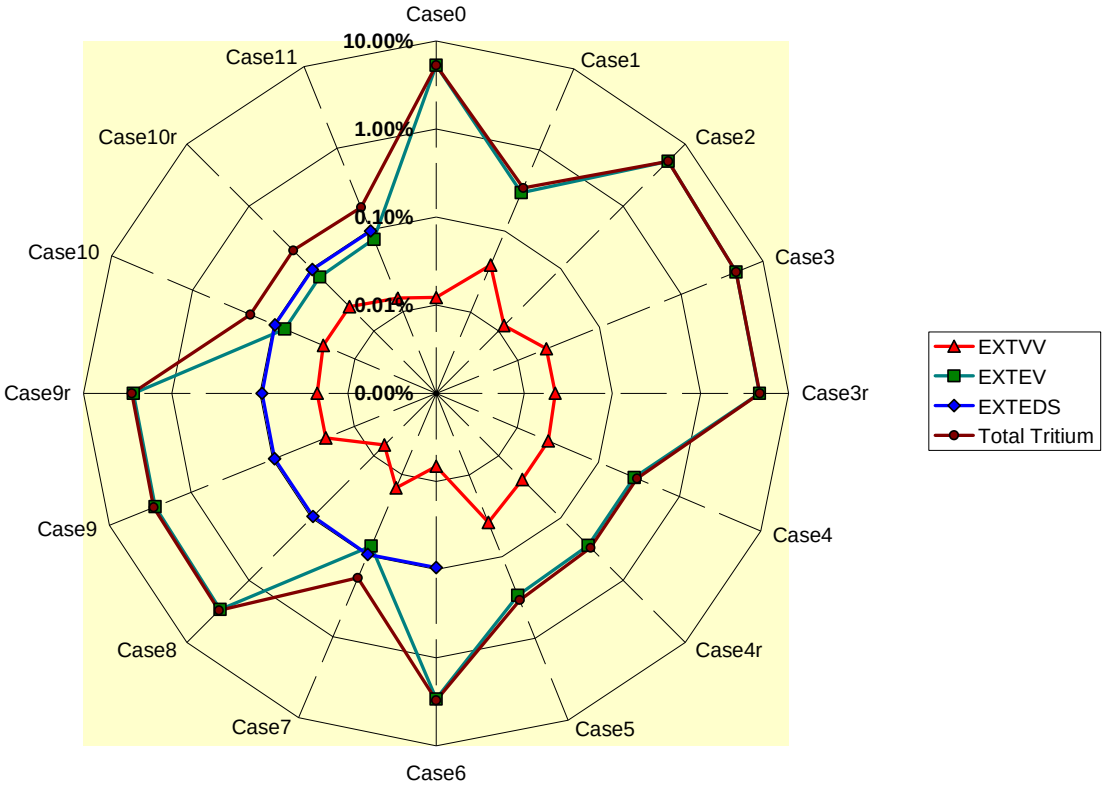

Figure 4.20: Parametrical analysis: Percentage of the total Tritium inventory released.

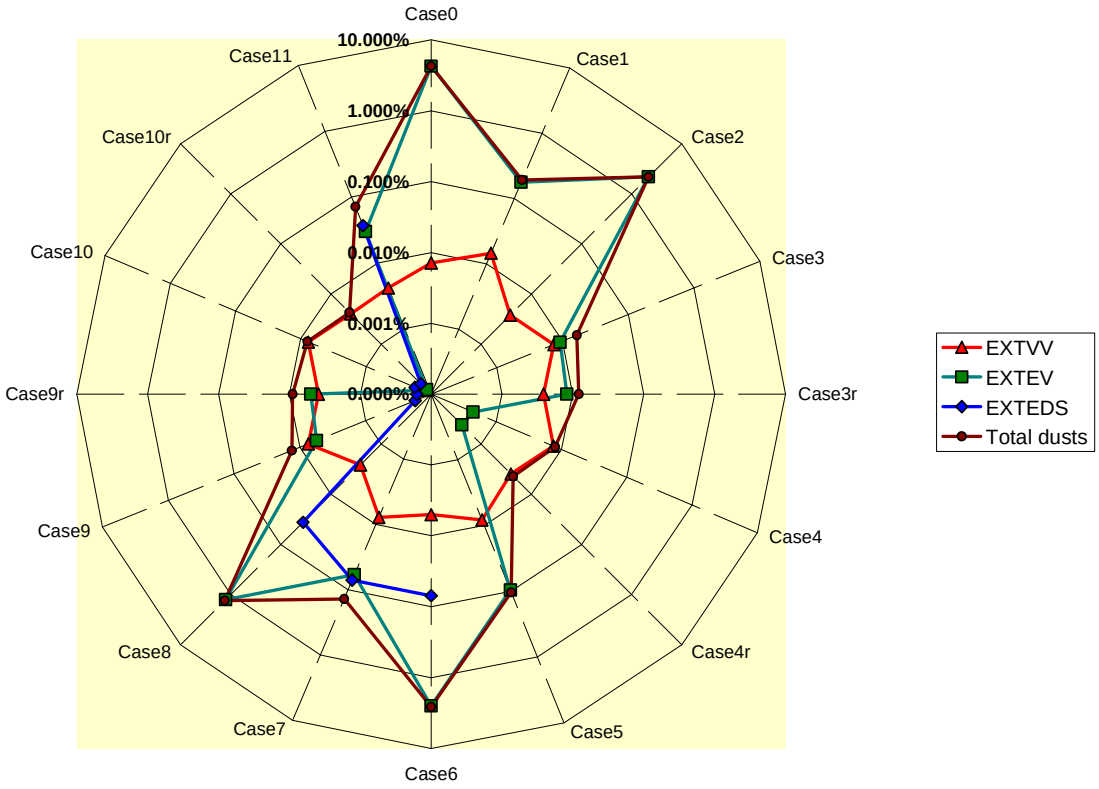

Figure 4.21: Parametrical analysis: Percentage of the total dust inventory released.

5. Conclusions

The scope of the present ECART analyses was to study the behaviour and the consequences in terms of radiological releases of the containment challenges for a beyond DBA sequence (LOFA + in-VV LOCA) for the PPCS Model B (Helium cooled).

The ECART code was able to provide a good qualitative and quantitative description of the 24 hours accident scenario. Furthermore, it was able to contemporarily assess the environmental releases of both dusts and tritium gas, considering also the possible retention phenomena and new mitigative modifications of the PPCS confinement design.

So, these analyses allowed to test the proposed PPCS Model B confinement concept and, at the same time, highlighted the following relevant issues, which will require, in the next future, more refined investigations:

- *Dust resuspension inside the VV*; the "mobilization fraction" of the deposited dusts after the start of the helium coolant release into the VV should be better investigated, as it is a fundamental parameter quite linearly influencing the subsequent transport processes and the external releases;
- *EV daily leakage*; in fact, **to avoid too large tritium gas releases, the daily leakages from the EV have to be carefully assessed**, implementing technical solutions for the confinement having lower leakage rates (a stainless steel liner, for example).

Particular new objectives undergoing and future activities are challenging, mainly due to the large radioactive releases predicted, but feasible solutions (i.e., the DS or the scrubber implementation) have been just identified:

- advice the **necessity of the implementation of a DS** for the EV atmosphere, with characteristics to be further analysed starting from the data of GSSR, to reduce the external releases but also to reduce the very large tritium mass still present inside the EV at the end of the 24 hours transient;
- advice the **necessity of the implementation of a pool scrubber**, after the RD between the VV and the EV, with design characteristics to be determined, to obtain a strong reduction of the dust external releases;

- **strong reduction of the EV daily leakages** from the initial value of 75% of the EV free volume; also the modelling of these daily leakages as a function of the differential pressure has to be further investigated; in fact, the dependence of the leakage flow-rate from the square root of the differential pressure is only applicable for a turbulent flow while, for small leakages rates, laminar flow conditions are more realistic, with a linear dependence of the mass flow-rate from the differential pressure.

Summarising, the main conclusions of the present work on the PPCS Model B confinement utilising the integrated ECART code are:

a) identification of the most relevant phenomena influencing the "containment function", including the external radioactive releases, for the proposed design of the PPCS Model B confinement;

b) **achieving the final goal to demonstrate that:**

   - **the overpressure in the VV and in the EV is safely mitigated under the design pressure, and**
   - **the external tritium and dusts radioactive releases could be mitigate with ad hoc design changes,** also proposed in the present work**.**

A final consideration is about the ECART code. A large number of sensitivity runs (16) was required to perform this job but, thanks to the quite short consumed CPU time an integrated thermal-hydraulics/aerosol transient lasting 24. hours (about 2,400. s of CPU time – see Figure 5.1 - for, on a personal computer equipped with a Pentium© IV processor at 2500 MHz), it was possible in a reasonable time.

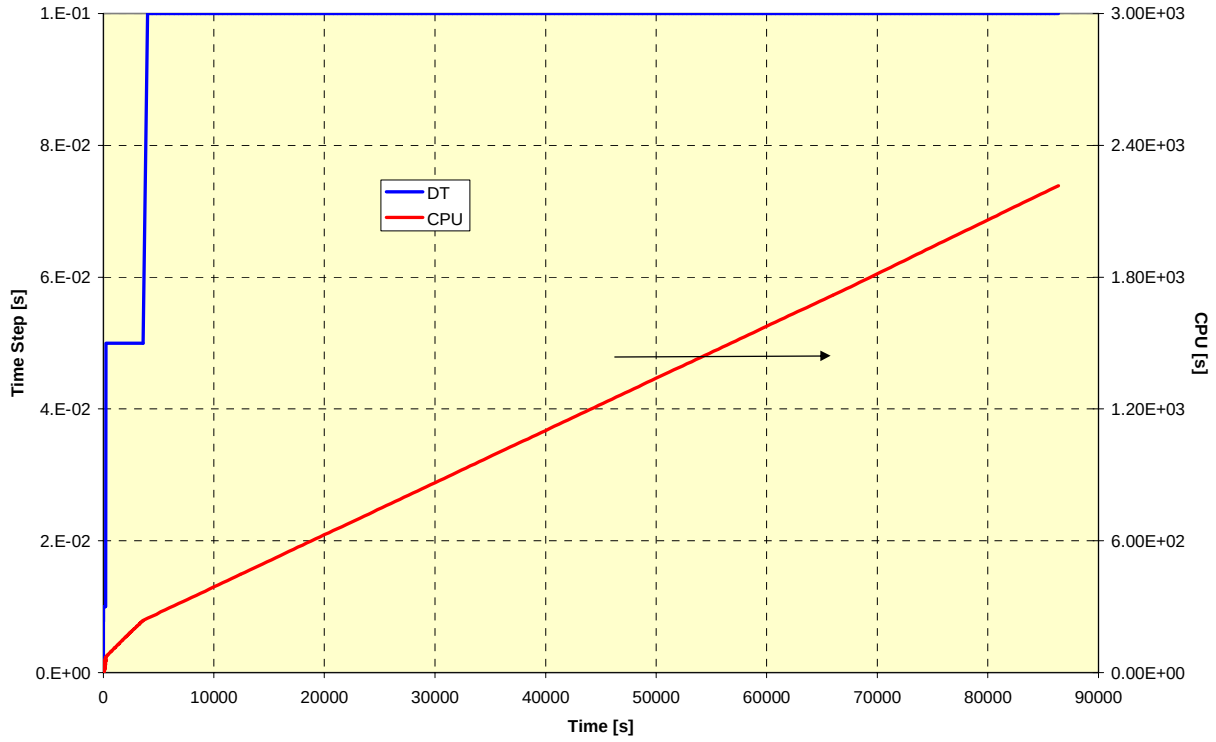

Figure 5.1: Time step and CPU time.

REFERENCES

[Alleman 1985] R.T. Alleman, "*Status of Validation of the SPARC Computer Code - Review of the Status of Validation of the Computer Codes Used in the Severe Accident Source Terms Reassessment Study (BMI-2104)*", Chap XII, Rep. ORNL/TM-8842, April 1985.

[Ambrosini, 1995] W. Ambrosini, G. Fruttuoso, F. Oriolo, F. Parozzi, *"Thermal-Hydraulic Modelling in Support to Severe Accident Radionuclide Transport"*, Nuclear Technology, Vol. 112, No. 2, Nov. 1995, pp. 239-249.

[Boerrigter, 2002] H. Boerrigter, "*Gas Cleaning at ECN: Lessons learned and results achieved*", ECN Biomass contribution to the GasNET & IEA Bioenergy Agreement Meeting, Strasbourg, France, 2-3 October 2002

[Brockmann 1985] J.E. Brockmann, "*Range of Possible Dynamic and Collision Shape Factors*", Report SAND84 - 0410, Vol. 2, App. F, February 1985.

[Cambi, 2002] G. Cambi, S. Paci, F. Parozzi, M.T. Porfiri, "*Ex-Vessel Break in ITER Divertor Cooling Loop Analysis with the ECART Code*", 22nd Symposium on Fusion Technology, SOFT 22, Helsinki (FIN), September 9 - 13, 2002,

[Di Pace, 2002] L. Di Pace, T. Pinna, M.T. Porfiri, "*Accident Description for Power Plant Conceptual Study*", ENEA Report FUS-TN-SA-SE-R-47, Rev. 1, Frascati, September 2002.

[ENEA, 2003] First Meeting of the Contract No. 03/58/30/AA between ENEA FUS and DIMNP of Pisa University, ENEA Frascati, July 18th, 2003.

[Honda, 2000] T. Honda, H.W. Bartels, "*Accident Analysis Specifications for GSSR*", (AAS-3) G 81 RI 3 00-02-29 W 0.1, 29 February, 2000.

[Jones, 2001] A.V. Jones, et al., "*Validation of Severe Accident Codes Against PHEBUS FP for Plant Applications (PHEBEN2)*", FISA 2001 Meeting on EU Severe Accident Researches, Luxemburg, 12 - 14 November 2001.

[Hermsmeyer, 2002] S. Hermsmeyer, e- mail October 24, 2002.

[Meloni, 2002] P. Meloni, ENEA Bologna, private communication, August 1st, 2002.

[Meloni, 2003] P. Meloni, M.T. Porfiri, ENEA FUS Frascati, private communication, e-mail January 13, 2003.

[NEA, 2000] *"Insight into the Control of the Releases of I, Cs, Sr and other Fission Products in the Containment by Severe Accident Management"*, OECD Report NEA/CSNI/R(2000)9, March 30th, 2000.

[Oehlberg 1985] R. Oehlberg, "*Radionuclide Scrubbing in Water Pools - Vol. 1: Gas-Liquid Hydrodynamics*", Rep. EPRI NP-4154 (project 2117-1), August 1985.

[Owczarski 1983] P.C. Owczarski, R.I. Schreck, A.K. Postma, "*Technical Bases and User's Manual for the Prototype of a Suppression Pool Aerosol Remove Code (SPARC)*", Pacific Northwest Lab., Rep. NUREG/CR-3317, PNL-4742, May 1983.

[Oriolo, 1998] F. Oriolo, S. Paci, *"DCMN Calculations for the ICE Facility"*, Atti del Dipartimento di Costruzioni Meccaniche e Nucleari, Pisa, DCMN 016 (98).

[Paci, 2000] S. Paci, *"DIMNP Pre-Test Calculations for the EVITA Facility Using the ECART Code"*, Atti del Dipartimento di Ingegneria Meccanica, Nucleare e della Produzione, Pisa, DIMNP 017 (00).

[Paci, 2003] S. Paci, *"ECART Analysis of an In-Vessel Break in the First Wall of the Power Plant Conceptual Study"*, Atti del Dipartimento di Ingegneria Meccanica, Nucleare e della Produzione, DIMNP 001 (03).

[Parozzi, 1997 a] F. Parozzi et al., *"ECART USER MANUAL Part 1: User's Guidance"*, ENEL Nuclear Energy Division Report, Milan, May 1997.

[Parozzi, 1997 b] F. Parozzi et al., *"ECART USER MANUAL Part 2: Code Structure and Theory"*, ENEL Nuclear Energy Division Report, Milan, May 1997.

[Parozzi, 2002] F. Parozzi, S. Paci, *"Relevant Aerosol and Chemistry Phenomena Expected in ITER-FEAT under Accident Conditions and Pre-test Simulations of STARDUST Experimental Facility Performed with the ECART Code"*, CESI Final Report A2/038115, CESI Milano, Ottobre 2002

[Porfiri, 2002] M.T. Porfiri, ENEA FUS Frascati, private communication, August 7th, 2002.

[Porfiri, 2003] M.T. Porfiri, ENEA FUS Frascati, private communication, e- mail August 25th, 2003.

[Porfiri, 2003a] M.T. Porfiri et alii, "*STARDUST Experiment : Set Up of the Facility for the Dust Mobilization*" ENEA FUS Frascati Report FUS-TN-SA-SE-R-75, June 2003.

[SPARC 1988a] "*SPARC Code Listing*", draft version received by ENEL from ENEA (Italy), August 1988.

[SPARC 1988b] "*SPARC Code Listing*", version included in the Source Term Code Package, received by ENEL from the Battelle Columbus Lab., October 1988.

[Wright, 1994] A.L. Wright, "*Primary System Fission Product Release and Transport: a State of the Art Report to the CSNI*", US NRC NUREG/CR-6193, NEA/CSNI/R (94), June 1994.

Appendix: ECART Input Deck for Case 3

```
PPCS new Athena data (July 03) Case 3
S. Paci - DIMNP Pisa University
$
$    2 volumes + 2 BE
$    Vol EV 68000.0 - 1 structure for th (thick 400. mm) 3 part (lat,floor&ceil
$    Vol VV  3830.0 - adiabatic FW - DV htc 1.E4 (?)
$    No Vol PS   adiabatic with insulant (area 3600 m**2)
$    4 heat structures: VV (FW & DV)
$                       EV 0.1 area for th
$                       no PS in VV
$    2 BE for leakages from VV and EV
$    0 implicit junctions
$    4 explicit junction (2 lkgs, He injection & Rupture Disk 0.2 m*2)
$    no decay heat in FW e DV for 0.01 m
$    lkg EV 75%
$    no DS = 2 EJ + 2 BE
$    scrubber attivato
$    no multicomponente
$    I iterazione x scrubber
$
$====================== GENERAL PARAMETERS ============================
$
2    $ IPROG
0    $ NREST
4    $ NONCN  Non-condensable gases (N2, O2, He, CO2)
2    $ NVOL   Num. volumes
4    $ NBE    back-environment
0    $ NJUN   implicit junctions
6    $ NSPIL  explicit junctions
4    $ NSTRUC
2    $ NMAT   Num. materials
0    $ NTABP  Num. power tables (FW)
$
$
$===============  GAS COMPONENTS ======================================
$
  'N2'   $   Nitrogen
  'O2'   $   Oxygen
  'HE'   $   Helium
  'CO2'  $   Carbon Dioxide
$
$------------ Primary VOLUME T-H DATA (only He) -------------------------
$   CHVOL
$   'PS'
$ ROUGHV               PHVOL                            IAXIS
$  1.E-04               0.5                                0
$ AHOR                 ALNGTH           PHIVOL          IGEOM
$  1.0                   344.6             0.              0
$ IOPT
$    1
$ PVOL          TLVOL    XLVOL   TGVOL    XGVOL   ALGLEV
$  8.0E6         473.15     0.    673.15      1.      0.0
$  ANVOL
$  0.  0.  0.999  0.
$
$------------ VV VOLUME T-H DATA (steam only) ---------------------------
$   CHVOL
   'VV'
$ ROUGHV               PHVOL                            IAXIS
  1.E-04               17.970                             0
```

```
$ AHOR                  ALNGTH            PHIVOL          IGEOM
  25.697                149.045                0.              0
$ IOPT
    1
$ PVOL          TLVOL     XLVOL    TGVOL     XGVOL    ALGLEV
  6.2E2         473.15      0.     473.15       1.       0.0
$  ANVOL
  0.  0.  0.  0.
$
$------------ EV VOLUME T-H DATA (air ) ---------------------------------
$   CHVOL
   'EV'
$ ROUGHV                PHVOL                               IAXIS
  1.E-04                146.160                                 1
$ VNEXT     FAREXT    VNINT    FARINT    NVVOL
  1.          1.        0.       1.       4
$ ZVOL     AEXT     BEXT     AINT      BINT
  0.        100.0      1.       0.        0.
  1.999     100.0      1.       0.        0.
  2.       1700.0      1.       0.        0.
  42.      1700.0      1.       0.        0.
$ IOPT
    1
$ PVOL          TLVOL     XLVOL    TGVOL     XGVOL    ALGLEV
  0.9E5        303.15      0.     303.15    1.       0.999
$  ANVOL
  0.77 0.20  0.  0.02
$
$
$================ BACK ENVIRONMENT DATA ==============================
$
$---------- Environment VV ------------------
$   CHBE         NVBE     CHCNBE      TCONBE
  'EXTVV'          2      ' -- '       1.E10
$   TBE      PBET      TLBET    TGBET    ALGBET    ANBET (N2)
  -1000.   1.013E5   293.15   293.15     1.0      0.77   0.20   0. 0.02
   1.E6    1.013E5   293.15   293.15     1.0      0.77   0.20   0. 0.02
$
$---------- Environment EV ------------------
$   CHBE         NVBE     CHCNBE      TCONBE
  'EXTEV'          2      ' -- '       1.E10
$   TBE      PBET      TLBET    TGBET    ALGBET    ANBET (N2)
  -1000.   1.013E5   293.15   293.15     1.0      0.77   0.20   0. 0.02
   1.E6    1.013E5   293.15   293.15     1.0      0.77   0.20   0. 0.02
$
$---------- Environment DS ------------------
$   CHBE         NVBE     CHCNBE      TCONBE
  'EXTEDS'         2      ' -- '        1.E10
$   TBE      PBET      TLBET    TGBET    ALGBET    ANBET (N2)
  -1000.   1.013E5   293.15   293.15     1.0      0.76   0.20   0.02 0.015
   1.E6    1.013E5   293.15   293.15     1.0      0.76   0.20   0.02 0.015 $
$
$---------- Environment Clean ------------------
$   CHBE         NVBE     CHCNBE      TCONBE
  'EXTCLN'         2      ' -- '        1.E10
$   TBE      PBET      TLBET    TGBET    ALGBET    ANBET (N2)
  -1000.   1.013E5   293.15   293.15     1.0      0.76   0.20   0.02 0.015
   1.E6    1.013E5   293.15   293.15     1.0      0.76   0.20   0.02 0.015 $
$
$
$================== EXPLICIT JUNCTION DATA ============================
$
$---------- VV Leak ----------------------
$   CHSPIL
   'VVLKG'
```

```
$   ITYSPI   CHFRSP     CHTOSP    ZFRSPI   DZFRSP  ZTOSPI  DZTOSP
        2   'EXTVV'      'VV'      0.1    0.00    2.86     0.01
$   THTFRS    PHIFRS    THTTOS     PHITOS
       0.         0.       0.         0.
$   IHOMFS    IHOMTS    ISCRUB
        0          0         0
$   NVSPIL
      12
$   PRESPT  WGSPIT     PRFSPT   TLSPIT  TGSPIT  ALGSPT  ANSPIT
        0.   0.0       1.1E5    573.    573.    0.0     0.0 0.0 1.0 0.0
    1.013e5  0.0       1.1E5    573.    573.    0.0     0.0 0.0 1.0 0.0
    1.020e5 -1.113E-04 1.1E5    573.    573.    0.0     0.0 0.0 1.0 0.0
    1.030e5 -1.734E-04 1.1E5    573.    573.    0.0     0.0 0.0 1.0 0.0
    1.050e5 -2.558E-04 1.1E5    573.    573.    0.0     0.0 0.0 1.0 0.0
    1.100e5 -3.923E-04 1.1E5    573.    573.    0.0     0.0 0.0 1.0 0.0
    1.200e5 -5.571E-04 1.2E5    573.    573.    0.0     0.0 0.0 1.0 0.0
    1.300e5 -7.124E-04 1.3E5    573.    573.    0.0     0.0 0.0 1.0 0.0
    1.400e5 -8.273E-04 1.4E5    573.    573.    0.0     0.0 0.0 1.0 0.0
    1.500e5 -9.280E-04 1.5E5    573.    573.    0.0     0.0 0.0 1.0 0.0
    1.600e5 -1.019E-03 1.6E5    573.    573.    0.0     0.0 0.0 1.0 0.0
    2.000e5 -1.330E-03 2.0E5    573.    573.    0.0     0.0 0.0 1.0 0.0
$
$---------- EV Leak ----------------------
$   CHSPIL
   'EVLKG'
$   ITYSPI   CHFRSP     CHTOSP    ZFRSPI   DZFRSP  ZTOSPI  DZTOSP
        2   'EXTEV'      'EV'      0.1    0.00    20.0     0.01
$   THTFRS    PHIFRS    THTTOS     PHITOS
       0.         0.       0.         0.
$   IHOMFS    IHOMTS    ISCRUB
        0          0         0
$   NVSPIL
      11
$   PRESPT  WGSPIT     PRFSPT   TLSPIT  TGSPIT  ALGSPT  ANSPIT
        0.   0.0       1.1E5    573.    573.    0.0     0.0 0.0 1.0 0.0
    1.013e5  0.0       1.1E5    573.    573.    0.0     0.0 0.0 1.0 0.0
    1.020e5 -6.695E-02 1.1E5    573.    573.    0.0     0.0 0.0 1.0 0.0
    1.030e5 -1.043E-01 1.1E5    573.    573.    0.0     0.0 0.0 1.0 0.0
    1.050e5 -1.539E-01 1.1E5    573.    573.    0.0     0.0 0.0 1.0 0.0
    1.100e5 -2.360E-01 1.1E5    573.    573.    0.0     0.0 0.0 1.0 0.0
    1.200e5 -3.460E-01 1.2E5    573.    573.    0.0     0.0 0.0 1.0 0.0
    1.300e5 -4.287E-01 1.3E5    573.    573.    0.0     0.0 0.0 1.0 0.0
    1.400e5 -4.978E-01 1.4E5    573.    573.    0.0     0.0 0.0 1.0 0.0
    1.500e5 -5.584E-01 1.5E5    573.    573.    0.0     0.0 0.0 1.0 0.0
    1.600e5 -6.198E-01 1.6E5    573.    573.    0.0     0.0 0.0 1.0 0.0
$
$---------- He Injection -----------------
$   CHSPIL
$   'INLET'
$   ITYSPI   CHFRSP     CHTOSP    ZFRSPI   DZFRSP  ZTOSPI  DZTOSP
$        4   'PS'       'VV'        0.1    0.00    2.86     0.01
$   THTFRS    PHIFRS    THTTOS     PHITOS
$       0.         0.       0.         0.
$   IHOMFS    IHOMTS    ISCRUB
$         0          0         0
$   ICRTSP  TOPSPI  TCLSPI  POPSPI  PCLSPI  DZTLIN  PREFSP
$       -1    0.0    1.E12   1.E12   1.E-6    0.0     0.0
$   CTOSP   TAUSP
$     0.0     0.0
$   AREFF     CDL     CDV
$    7.36e-4   1.0     0.9435
$
$   CHSPIL
   'INLET'
$   ITYSPI   CHFRSP     CHTOSP    ZFRSPI   DZFRSP  ZTOSPI  DZTOSP
```

```
         1  '&ENVIR'    'VV'          0.     0.01    0.50     0.01
$   THTFRS    PHIFRS    THTTOS     PHITOS
       0.         0.        0.         0.
$   IHOMFS    IHOMTS    ISCRUB
         0          0         0
$   NVSPIL
      22
$   TSPIL   WGSPIT  PRFSPT    TLSPIT  TGSPIT  ALGSPT  ANSPLT
-100.0 0.000000  7897622.0  619.9221    619.9221 1.  0. 0. 1. 0.
 0.0   0.000000  7927478.0  872.2664    872.2664 1.  0. 0. 1. 0.
 1.0   3.415121  7914242.0  841.3976    841.3976 1.  0. 0. 1. 0.
 2.0   3.425754  7890068.0  838.4251    838.4251 1.  0. 0. 1. 0.
 5.0   3.393125  7818214.0  839.2984    839.2984 1.  0. 0. 1. 0.
 10.0  3.339629  7714240.0  843.4548    843.4548 1.  0. 0. 1. 0.

 25.0  3.233578  7439894.0  836.6774    836.6774 1.  0. 0. 1. 0.
 50.0  3.131688  7104952.0  813.4542    813.4542 1.  0. 0. 1. 0.
100.0  2.970279  6554848.0  769.6801    769.6801 1.  0. 0. 1. 0.
150.0  2.787631  6016233.0  736.1591    736.1591 1.  0. 0. 1. 0.
200.0  2.598292  5514647.0  711.8902    711.8902 1.  0. 0. 1. 0.
300.0  2.221005  4614104.0  682.0750   682.0750 1.  0. 0. 1. 0.
400.0  1.873934  3847002.0  666.0308    666.0308 1.  0. 0. 1. 0.
500.0  1.570605  3200978.0  656.4331    656.4331 1.  0. 0. 1. 0.
650.0  1.199027  2427786.0  647.9221    647.9221 1.  0. 0. 1. 0.
750.0  0.999258  2017715.0  644.3546    644.3546 1.  0. 0. 1. 0.
1000.0 0.627209  1268715.0  646.6421    646.6421 1.  0. 0. 1. 0.
1250.0 0.391828   796054.4  652.3113    652.3113 1.  0. 0. 1. 0.
1500.0 0.245082   499842.9  657.3609    657.3609 1.  0. 0. 1. 0.
1972.2 0.075995   215720.8  664.2102    664.2102 1.  0. 0. 1. 0.
1973.0 0.000000   215720.8  664.2102    664.2102 1.  0. 0. 1. 0.
1.E6   0.000000   215720.8  664.2102    664.2102 1.  0. 0. 1. 0.
$
$---------- Rupture Disk ------------------
$   CHSPIL
   'RD'
$   ITYSPI   CHFRSP      CHTOSP     ZFRSPI   DZFRSP  ZTOSPI  DZTOSP
         4  'VV'         'EV'       5.6      0.      0.1      0.
$   THTFRS    PHIFRS    THTTOS     PHITOS
      90.        0.       90.         0.
$   IHOMFS    IHOMTS    ISCRUB
         0          0         1
$   ICRTSP  TOPSPI  TCLSPI  POPSPI  PCLSPI  DZTLIN  PREFSP
        -1   1.E12   1.E12   1.0E5   1.E-6    3.0     0.0
$   CTOSP   TAUSP
     0.0     0.0
$   AREFF     CDL     CDV
    0.2       1.0     1.0
$
$------ estraction pump for detritiator -----------------
$       (closed, to be opened when EV pressure increases)
$   CHSPIL
   'EDSOUT'
$   ITYSPI   CHFRSP      CHTOSP     ZFRSPI   DZFRSP  ZTOSPI  DZTOSP
         3   'EXTEDS'     'EV'      20.      0.       20.       0.
$   THTFRS    PHIFRS    THTTOS     PHITOS
      -90.        0.      -90.         0.
$   IHOMFS    IHOMTS    ISCRUB
         0          0         0
$   WGSPIT        PRFSPT   TLSPIT  TGSPIT  ALGSPT   ANSPLT
      -3.0       1.013E5   303.    303.       1.    0.76 0.20 0.02 0.015
$   TOPSPI  TCLSPI    POPSPI   PCLSPI
    120.E5    1.E12    1.E12    1.E12
$
$------ inlet pump for detritiator (air ingress) ---
$       (closed, to be opened when DS starts)
```

```
$   CHSPIL
   'EDSIN'
$   ITYSPI   CHFRSP      CHTOSP     ZFRSPI   DZFRSP  ZTOSPI  DZTOSP
         3  'EXTCLN'     'EV'       20.      0.      20.       0.
$   THTFRS    PHIFRS    THTTOS     PHITOS
      -90.        0.      -90.         0.

$   IHOMFS    IHOMTS    ISCRUB
         0         0         0
$   WGSPIT        PRFSPT   TLSPIT  TGSPIT  ALGSPT   ANSPLT
       3.0       1.013E5   323.    323.      1.    0.76 0.2 0.02 0.015
$   TOPSPI  TCLSPI    POPSPI   PCLSPI
    120.E5    1.E12     1.E12    1.E12
$
$
$================== HEAT STRUCTURE DATA =========================
$
$---------- PS Wall (EU) in VV  ---------------------
$   CHSTRU
    '000'
$    ITIPO        RI      NREG     AREAI    AREAE    CHVINT    CHVEXT
         1        0.5        1     1.e-3    1.e-3    'VV'      '&ENVIR'
$      DHI       DHE    HFOULI    HFOULE     FACWI     FACWE
       1.        1.     1.E10     1.E10       1.        1.
$    ZBOTI     ZTOPI     ZBOTE     ZTOPE
      0.0       1.0       0.0       1.0
$    NVENV
       2
$    TENV    TMENVT    HENVT
    -1000.    573.    1.E4
     1.E6     573.    1.E4
$    DREG     NINREG   FQREG  ITPREG IMREG
     0.050      5        0.      0     1
$
$---------- VV Wall FW  (EU) ---------------------
$   CHSTRU
    '001FW'
$    ITIPO        RI      NREG     AREAI    AREAE    CHVINT    CHVEXT
         1       0.0        1      1253.    1253.    'VV'      '&ENVIR'
$      DHI       DHE    HFOULI    HFOULE     FACWI     FACWE
      5.72      5.72     1.E10     1.E10       1.        1.
$    ZBOTI     ZTOPI     ZBOTE     ZTOPE
      0.0       5.72       0.0      5.72
$    NVENV
       11
$    TENV    TMENVT    HENVT
       -0.1  1150.    1.E5
        0.   1150.    1.E5
        1.   1450.    1.E5
        5.   1200.    1.E5
       15.   1150.    1.E5
       70.   1000.    1.E5
      200.    800.    1.E5
      500.    700.    1.E5
     1000.    650.    1.e5
     2000.    680.    0.0
      1.E5    680.    0.0
$    DREG     NINREG   FQREG  ITPREG IMREG
     0.001        4        0.      0     1
$     0.56      28        0.      0     1
$
$---------- VV Wall DV  (EU) ---------------------
$   CHSTRU
    '001DV'
$    ITIPO        RI      NREG     AREAI    AREAE    CHVINT    CHVEXT
```

```
         1         0.0        1        391.     391.   'VV'       '&ENVIR'
$       DHI        DHE     HFOULI     HFOULE     FACWI      FACWE
       5.72        5.72     1.E10      1.E10        1.         1.
$     ZBOTI      ZTOPI      ZBOTE      ZTOPE
       0.0         0.0        0.0        0.0
$     NVENV
         4
$     TENV     TMENVT     HENVT
     -1000.     673.     1.E4
         0.     673.     1.E4
         0.01   673.     1.E4
      1.E6      673.     1.E4
$     DREG      NINREG    FQREG   ITPREG IMREG
      0.01       4          0.       0      1
$     0.49      25          0.       0      1
$
$---------- EV Wall  (concrete) ----------------------
$    CHSTRU
     '002'
$     ITIPO         RI       NREG      AREAI     AREAE     CHVINT     CHVEXT
          1     23.262          1     9246.412 9246.412 'EV'       '&ENVIR'
$       DHI        DHE     HFOULI     HFOULE     FACWI      FACWE
      46.52      46.52      1.E10      1.E10        1.         1.
$     ZBOTI      ZTOPI      ZBOTE      ZTOPE
       0.0        40.0        0.0       40.0
$     NVENV
         2
$     TENV     TMENVT     HENVT
     -1000.     293.15     0.0
      1.E6      293.15     0.0
$     DREG      NINREG    FQREG   ITPREG IMREG
      0.400       20          0.       0      2
$
$
$================= MATERIAL DATA ======================================
$
$----------------- Material 1 - EUROFER -------------------------
$
$$$ Thermal conductivity
$
$ NAK (number of rows)
  4
$ AKT [K]     AKV [W/(mK)]
  293.        31.3
  873.        33.0
 1073.        30.
 2000.        30.
$
$$$ Heat capacity
$
$ NVHC (number of rows)
  7
$ VHCT [K]    VHCV [J/(m3K)]
  293.        3.494E6
  527.        4.492E6
  823.        5.320E6
  973.        6.755E6
 1033.        9.009E6
 1073.        6.263E6
 2000.        6.263E6
$
$----------------- Material 2 - Concrete -------------------------------
$
$$$ Thermal conductivity
$
```

```
$ NAK (number of rows)
  4
$ AKT [K]     AKV [W/(mK)]
  250.        1.1
  500.        0.7
  1000.       0.5
  2600.       0.3
$
$$$ Heat capacity
$
$ NVHC (number of rows)
  4
$ VHCT [K]    VHCV [J/(m3K)]
  250.        2340000.
  500.        2614000.
  1000.       2900350.
  2600.       3000000.
$
$================== NO HEAT STRUCTURE POWER DATA ======================
$
$============================ NO PUMP DATA ============================
$    NPUMP
         0
$
$====================== ADVANCEMENT CONTROL DATA ======================
$
$    TEND             NFREQ    NPLTH
     86400.              6       22
$
$    TSTEA     DTSTEA     DTSTOU     NJUDEL     NSPDEL     ICOUST
      -.1      1.E-1         1.        0          0          1
$    TFREQ       DTUP       DTLW     DTTROU     DTTRPL     ICOURT
        0.      1.0E-2     1.E-8        2.0      0.2        1
       50.      1.0E-2     1.E-8        2.0      0.2        1
      100.      1.0E-2     1.E-8       10.0      1.0        1
      200.      1.0E-2     1.E-8       20.       2.0        1
     3600.      5.0E-2     1.E-7      200.      20.0        1
    86400.      1.0E-1     1.E-6     1200.     400.0        1
$
$CHPLOT       CHPLO1      INDPL2     CONVFP    NWCHPL
'PVOL'       'VV'         1          0       'PS press'
'PVOL'       'VV'         1          0       'VV press'
'PVOL'       'EV'         1          0       'EV press'
'ANVOL'      'VV'         3          0       'He VV fr'
'ANVOL'      'EV'         3          0       'He EV fr'
'AMGVOL'     'VV'         3          0       'gas mass VV'
'AMGVOL'     'EV'         3          0       'gas mass EV'
'TGVOL'      'VV'         1          0       'PS T'
'TGVOL'      'VV'         1          0       'VV T'
'TGVOL'      'EV'         1          0       'EV T'
'T'          '000'        1          0       'PS Tw int'
'T'          '001FW'      1          0       'FW Tw int'
'T'          '001DV'      1          0       'DV Tw int'
'T'          '002'        1          0       'EV Tw int'
'T'          '000'        6          0       'PS Tw ext'
'T'          '001FW'      5          0       'FW Tw ext'
'T'          '001DV'      5          0       'DV Tw ext'
'T'          '002'        3          0       'EV Tw ext'
'WGSPIL'     'INLET'      0          0       'He release'
'WGSPIL'     'RD'         0          0       'RD flow'
'WGSPIL'     'VVLKG'      0       -1.0       'VV leak'
'WGSPIL'     'EVLKG'      0       -1.0       'EV leak'
$
$
$=====================================================================
```

```
$  AEROSOL AND VAPOR TRANSPORT SECTION
$=====================================================================
$
$ Dust (W & SS) and T2 in VV
$ AMMD dust 1.492 micron (from W data of SADL ?)
$ 1 structure for EV (but with floor & ceiling)
$
$
$$$     CONTROL DATA AND PROGRAM CONSTANTS
$
2         $  IUNIT
0         $  KOMAD
0         $  IPCOMP   multi-component
33        $  ISOLV
0         $  ICOND
$
4         $  NK (T2, W, SS + H2O)
0         $  NRADIS (decay heat elements)
5         $  NSTRX
20        $  NSMAX (default=20)
10        $  NSTP  (default=1)
10        $  NAPTP (default=1)
1         $  NORSET
53        $  NPLAV
$
0.        $  START TIME   (s)
0.        $  END TIME      "
0.0       $  DELTA T MIN   "
10.0      $  DELTA T MAX   "
-1.       $  DELTA T PRINT "
0.        $  DELTA T PLOT  "
$
0.01      $  ETA1
0.0       $  ETA2
0.0       $  REL
0.0       $  EPSAER
0.        $  FLORC
$
$
$====== GEOMETRIC DATA FOR AEROSOL AND VAPORS TRANSPORT ===========
$
$===VOLUME 1 - VACVUP ================================================
'VV'          $  VOLNAM
0.0           $  VOL    (m3)   (cfr. TH)
0.0           $  VLENG  (m)    (cfr. TH)
3             $  NSTR
1             $  IHOVE         (0=VERTICAL, 1=HORIZONTAL)
0.            $  TCLOSE
0.            $  XCLOSE
$
$- STRUC 000 - PS wall -------------------------
0.            $  LENGTH     (m)    (cfr. TH)
0.            $  DIAME      (m)    (cfr. TH)
0.            $  FLOW AREA  (m2)   (cfr. TH)
0.0           $  SURFT      (m2)   (total dep. surface)
180.0         $  SURFC      (m2)   (ceiling surface)
180.0         $  SURFS      (m2)   (floor surface)
0.            $  OAF               (floor open fraction)
0             $  IFALB             (fall-back volume)
0.            $  SURFB      (m2)   (curved surface)
0.            $  RBEND      (m)    (curvature radius)
1             $  IPLUG             (0=mixed)
0. 0.         $  SAF1 & SAF2
0.            $  ROUGH      (m)
00110         $  ISTRUC            (t-h identification number)
```

```
0.0          $  ABSGAM
0            $  ISTGAM
0            $  MTYP
$

$- STRUC 002 - Vacuum Vessel wall -------
0.           $  LENGTH     (m)    (cfr. TH)
0.           $  DIAME      (m)    (cfr. TH)
0.           $  FLOW AREA  (m2)   (cfr. TH)
0.0          $  SURFT      (m2)   (total dep. surface effective)
852.536         $  SURFC      (m2)   (ceiling surface)
461.536         $  SURFS      (m2)   (floor surface)
0.           $  OAF               (floor open fraction)
0            $  IFALB             (fall-back volume)
0.           $  SURFB      (m2)   (curved surface)
0.           $  RBEND      (m)    (curvature radius)
0            $  IPLUG             (0=mixed)
0. 0.        $  SAF1 & SAF2
0.           $  ROUGH      (m)
00210        $  ISTRUC            (t-h identification number)
0.0          $  ABSGAM
0            $  ISTGAM
0            $  MTYP              (oxydation of Be walls)
$
$- STRUC 003 - Divertor --------
0.           $  LENGTH     (m)    (cfr. TH)
0.           $  DIAME      (m)    (cfr. TH)
0.           $  FLOW AREA  (m2)   (cfr. TH)
0.           $  SURFT      (m2)   (total dep. surface)
0.           $  SURFC      (m2)   (ceiling surface)
391.         $  SURFS      (m2)   (floor surface)
0.           $  OAF               (floor open fraction)
0            $  IFALB             (fall-back volume)
0.           $  SURFB      (m2)   (curved surface)
0.           $  RBEND      (m)    (curvature radius)
0            $  IPLUG             (0=MIXED, 1=PLUG)
0. 0.        $  SAF1 & SAF2
0.           $  ROUGH      (m)
00310        $  ISTRUC            (t-h identification number)
0.0          $  ABSGAM
0            $  ISTGAM

0            $  MTYP              (oxydation of W walls)
$
$===VOLUME 3 - EV =======================================
'EV'     $  VOLNAM
0.0          $  VOL     (m3)   (cfr. TH)
0.0          $  VLENG   (m)    (cfr. TH)
1            $  NSTR
1            $  IHOVE         (0=VERTICAL, 1=HORIZONTAL)
0.           $  TCLOSE
0.           $  XCLOSE
$
$- STRUC 004 - EV floor, ceiling & lat -------------------
40.00        $  LENGTH     (m)    (cfr. TH)
46.52        $  DIAME      (m)    (cfr. TH)
0.           $  FLOW AREA  (m2)   (cfr. TH)
9246.412     $  SURFT      (m2)   (total dep. surface effective)
1700.0       $  SURFC      (m2)   (ceiling surface)
1700.0       $  SURFS      (m2)   (floor surface)
0.           $  OAF               (floor open fraction)
0            $  IFALB             (fall-back volume)
0.           $  SURFB      (m2)   (curved surface)
0.           $  RBEND      (m)    (curvature radius)
0            $  IPLUG             (0=mixed)
```

```
0. 0.        $  SAF1 & SAF2
0.           $  ROUGH     (m)
00410        $  ISTRUC           (t-h identification number)
0.0          $  ABSGAM
0            $  ISTGAM
0            $  MTYP             (oxydation of Be walls)
$
$===VOLUME 4 - EXTERNAL VV ======================================
'EXTVV'      $  VOLNAM
1.E12        $  VOL    (m3)   (cfr. TH)
1.E3         $  VLENG  (m)    (cfr. TH)
0            $  NSTR
0            $  IHOVE         (0=VERTICAL, 1=HORIZONTAL)
0.           $  TCLOSE
0.           $  XCLOSE
$
$===VOLUME 4 - EXTERNAL EV ======================================
'EXTEV'      $  VOLNAM
1.E12        $  VOL    (m3)   (cfr. TH)
1.E3         $  VLENG  (m)    (cfr. TH)
0            $  NSTR
0            $  IHOVE         (0=VERTICAL, 1=HORIZONTAL)
0.           $  TCLOSE
0.           $  XCLOSE
$
$===VOLUME 5 - EXTERNAL DS ======================================
'EXTEDS'     $  VOLNAM
1.E12        $  VOL    (m3)   (cfr. TH)
1.E3         $  VLENG  (m)    (cfr. TH)
0            $  NSTR
0            $  IHOVE         (0=VERTICAL, 1=HORIZONTAL)
0.           $  TCLOSE
0.           $  XCLOSE$
$
$===VOLUME 6 - EXTERNAL CLEAN ===================================
'EXTCLN'     $  VOLNAM
1.E12        $  VOL    (m3)   (cfr. TH)
1.E3         $  VLENG  (m)    (cfr. TH)
0            $  NSTR
0            $  IHOVE         (0=VERTICAL, 1=HORIZONTAL)
0.           $  TCLOSE
0.           $  XCLOSE
$
$
$=========================================================================
$
$  POOL SCRUBBING ORIFICE DATA (RD INTO EV)
$
$0.505       $ DORF (DIAMETER OF A SINGLE ORIFICE)
0.01         $ DORF (DIAMETER OF A SINGLE ORIFICE)
1            $ ORNT (ORIENTATION =0 VERTICAL)
40000        $ NORF (NUMBER OF ORIFICES)
$=========================================================================
$
$
$$$    AEROSOL AND CHEMICAL SPECIES SECTION
$
$$$    CHEMICAL SPECIES (SN)
$
'H2O'         0  0  0  0        0.  0.  0.  0.   0. 0
'T2'          1  0  0  1        0.  0.  0.  0.   0. 0
'W'           0  1  1  1        0.  0.  0.  0.   0. 0
'&SS'         0  1  1  1     7900.  0.  0.  0.  56. 0
$
$$$     OPTION FLAGS (OPT, 9 ENTRIES FOR EACH VOLUME)
```

```
$reac  depos  fb  resus  cond/evap  print  agglom recir chem
$ 00      1    0     1         0        2      1      1     0   $ PS
 00       1    0     1         0        2      1      1     0   $ VV
 00       1    0     1         0        2      1      1     0   $ EV
 00       0    0     0         0        2      0      0     0   $ EXTVV
 00       0    0     0         0        2      0      0     0   $ EXTEV
 00       0    0     0         0        2      0      0     0   $ EXTEDS
 00       0    0     0         0        0      0      0     0   $ EXTCLN
$
$$$      SENSITIVITY MULTIPLIERS
0.       $  TOPP          TIME OF FULL POWER
0        $  IDROP         DROP FLAG
0.       $  RCRIN         CRITICAL RADIUS FOR STEAM CONDENSATION
0.       $  FTRAPB        PARTICLE TRAPPING BY CURVED SURFACES
0.2      $  FWDRY         DRY SHAPE FACTORS
0.7      $  FWWET         WET SHAPE FACTORS
0.0      $  FLRSP         LIQUID PHASE TO RESUSPENSION INHIBIT
0.0      $  SIGWAT        sigma for water as aerosol 2.6
0.0      $  RGGWAT        Rg    for water as aerosol 0.01 micron
0        $  LVEQ          LIQUID-VAPOR EQUILIBRIUM IN CHEMISTRY
0        $  NTOPT         ITERATIONS FOR CHEMICAL EQUILIBRIUM
6*0.     $  RFMFAC
6*0.     $  OXRFAC
$
$
$=========================================================================
$ T2 initial mass (1.001 kg in VV)

1 0 0 0 0 0

1.001 0. 0. 0. 0. 0. 0.  $ VV

$-------------------------------------------------------------------
$ W source (2.4 kg in VV)

1 0 0 0 0 0


0 1 0 0 0 0 0   $ W aerosol puff within VV

  4                                                  $ n. points
  0. 2.5   5.0   1.E6                                $ times
  0. 0.96  0.    0.                                  $ source rates
$-------------------------------------------------------------------
$ SS source (7.6 kg in VV)

1 0 0 0 0 0

0 1 0 0 0 0 0   $ SS aerosol puff within VV

  4                                                  $ n. points
  0. 2.5   5.    1.E6                                $ times
  0. 3.04  0.    0.                                  $ source rates
$
$=========================================================================
$$$$      AEROSOL DISTRIBUTION PARAMETERS

$ W aerosol source size distribution in vol VACV

1 0 0 0 0 0

 1              $ constant parameter
 0.             $ time
 2.0            $ geom st deviation
```

```
 1              $ constant parameter
 0.             $ time
 -1.492E-6        $ AMMD

$-------------------------------------------------------------------
$ SS aerosol source size distribution in vol VACV

1 0 0 0 0 0

 1              $ constant parameter
 0.             $ time
 2.0            $ geom st deviation

 1              $ constant parameter
 0.             $ time
 -1.492E-6        $ AMMD

$-------------------------------------------------------------------
$$$$     AEROSOL SHAPE AND POROSITY

20*1.0          $    CHI           DYNAMIC SHAPE FACTOR
20*1.0          $    GAMMA         COLLISION SHAPE FACTOR
4*0.5           $    POR           POROSITY FACTOR

$-------------------------------------------------------------------
$
$$$$     PLOTS (variable, volume, struct, specie, junct, mechanism)

$  Suspended mass  T2 -------------------
'MSUSP'   1   0  'T2'       0 0 1.e3  'T2 PS'
'MSUSP'   1   0  'T2'       0 0 1.e3  'T2 VV'
'MSUSP'   2   0  'T2'       0 0 1.e3  'T2 EV'
'MSUSP'   3   0  'T2'       0 0 1.e3  'T2 EXTVV'
'MSUSP'   4   0  'T2'       0 0 1.e3  'T2 EXTEV'

$  Suspended mass W   -------------------
'MSUSP'   1   0  'W'       0 0 1.e3  'W PS'
'MSUSP'   1   0  'W'       0 0 1.e3  'W VV'
'MSUSP'   2   0  'W'       0 0 1.e3  'W EV'
'MSUSP'   3   0  'W'       0 0 1.e3  'W EXTVV'
'MSUSP'   4   0  'W'       0 0 1.e3  'W EXTEV'

$  Suspended mass SS  -------------------
'MSUSP'   1   0  '&SS'       0 0 1.e3  'SS PS'
'MSUSP'   1   0  '&SS'       0 0 1.e3  'SS VV'
'MSUSP'   2   0  '&SS'       0 0 1.e3  'SS EV'
'MSUSP'   3   0  '&SS'       0 0 1.e3  'SS EXTVV'
'MSUSP'   4   0  '&SS'       0 0 1.e3  'SS EXTEV '

$  Retained mass W  -------------------
'CRET'    1   0  'W'       0 0 1.e3  'W Ret PS'
'CRET'    1   0  'W'       0 0 1.e3  'W Ret VV'
'CRET'    2   0  'W'       0 0 1.e3  'W Ret EV'

$  Retained mass SS  -------------------
'CRET'    1   0  '&SS'       0 0 1.e3  'SS Ret PS'
'CRET'    1   0  '&SS'       0 0 1.e3  'SS Ret VV'
'CRET'    2   0  '&SS'       0 0 1.e3  'SS Ret EV'

$  Suspended Concentration T2 -------------------
'CSUSP'   1   0  'T2'       0 0 1.e3  'T2 CSUSP PS'
'CSUSP'   1   0  'T2'       0 0 1.e3  'T2 CSUSP VV'
'CSUSP'   2   0  'T2'       0 0 1.e3  'T2 CSUSP EV'
'CSUSP'   3   0  'T2'       0 0 1.e3  'T2 CSUSP EXTVV'
'CSUSP'   4   0  'T2'       0 0 1.e3  'T2 CSUSP EXTEV'
```

```
$  Injected mass  T2 -------------------
'CINJ'    1    0   'T2'       0 0 1.e3   'CINJ T2 VV'
'CINJ'    2    0   'T2'       0 0 1.e3   'CINJ T2 EV '
'CINJ'    3    0   'T2'       0 0 1.e3   'CINJ T2 EXTVV'
'CINJ'    4    0   'T2'       0 0 1.e3   'CINJ T2 EXTEV'

$  Injected mass  W -------------------
'CINJ'    1    0   'W'       0 0 1.e3   'CINJ W VV'
'CINJ'    2    0   'W'       0 0 1.e3   'CINJ W EV'
'CINJ'    3    0   'W'       0 0 1.e3   'CINJ W EXTVV'
'CINJ'    4    0   'W'       0 0 1.e3   'CINJ W EXTEV'

$  Injected mass  &SS -------------------
'CINJ'    1    0   '&SS'       0 0 1.e3   'CINJ SS VV'
'CINJ'    2    0   '&SS'       0 0 1.e3   'CINJ SS EV'
'CINJ'    3    0   '&SS'       0 0 1.e3   'CINJ SS EXTVV'
'CINJ'    4    0   '&SS'       0 0 1.e3   'CINJ SS EXTEV'

$  Suspended mass  DS 99.9% -------------------
'MSUSP'    5    0   'T2'        0 0 1.   'T2 DS'
'MSUSP'    5    0   'W'         0 0 1.   'W DS'
'MSUSP'    5    0   '&SS'       0 0 1.   'SS DS'
$
'ZDCF'     0    0   ' '         4 0 1.   'DF'
$
$  AMMD Suspended -------------------
'AMMD'    1    0   ' '       0 0 1.   'AMMD VV'
'AMMD'    2    0   ' '       0 0 1.   'AMMD EV'
'AMMD'    3    0   ' '       0 0 1.   'AMMD EXTVV'
'AMMD'    4    0   ' '       0 0 1.   'AMMD EXTEV'
$
$  GSD Suspended -------------------
'SIGG'    1    0   ' '       0 0 1.   'GSD VV'
'SIGG'    2    0   ' '       0 0 1.   'GSD EV'
'SIGG'    3    0   ' '       0 0 1.   'GSD EXTVV'
'SIGG'    4    0   ' '       0 0 1.   'GSD EXTEV'
$
$  Aerosol flow in RD -------------------
'FLOWC' 0    0   'T2'        4 0 1.   'T2 in RD'
'FLOWC' 0    0   'W'         4 0 1.   'W in RD'
'FLOWC' 0    0   '&SS'       4 0 1.   'SS in RD'
$========================== END OF DATA ================================
$
```